

# Global Convergence of Iteratively Reweighted Least Squares for Robust Subspace Recovery

Gilad Lerman<sup>a</sup>, Kang Li<sup>b</sup>, Tyler Maunu<sup>c</sup>, Teng Zhang<sup>b</sup>

<sup>a</sup>*University of Minnesota*

<sup>b</sup>*University of Central Florida*

<sup>c</sup>*Brandeis University*

---

## Abstract

Robust subspace estimation is fundamental to many machine learning and data analysis tasks. Iteratively Reweighted Least Squares (IRLS) is an elegant and empirically effective approach to this problem, yet its theoretical properties remain poorly understood. This paper establishes that, under deterministic conditions, a variant of IRLS with dynamic smoothing regularization converges linearly to the underlying subspace from any initialization. We extend these guarantees to affine subspace estimation, a setting that lacks prior recovery theory. Additionally, we illustrate the practical benefits of IRLS through an application to low-dimensional neural network training. Our results provide the first global convergence guarantees for IRLS in robust subspace recovery and, more broadly, for nonconvex IRLS on a Riemannian manifold.

*Keywords:* Robust subspace recovery, iteratively reweighted least squares, dynamic smoothing, nonconvex optimization

---

## 1. Introduction

Many real-world datasets in computer vision, machine learning, and bioinformatics exhibit underlying low-dimensional structure that can be effectively modeled using subspaces (Basri and Jacobs, 2003; Hartley and Zisserman, 2003; Lerman et al., 2015; Ding et al., 2020; Li et al., 2022; Yu et al., 2024; Wang et al., 2024; Arous et al., 2024). A variety of methods have been proposed to estimate such a subspace. The most prevalent of these is Principal Component Analysis (PCA) (Pearson, 1901; Hotelling, 1933; Jolliffe, 1986), which finds the directions of maximum variance within a dataset. However, PCA is well-documented to be sensitive to outliers.

These limitations spurred research into robust variants of PCA that can handle outliers; see Lerman and Maunu (2018b) for a comprehensive review. We focus specifically on robust subspace

---

*Email addresses:* [lerman@umn.edu](mailto:lerman@umn.edu) (Gilad Lerman), [kang.li@ucf.edu](mailto:kang.li@ucf.edu) (Kang Li), [maunu@brandeis.edu](mailto:maunu@brandeis.edu) (Tyler Maunu), [teng.zhang@ucf.edu](mailto:teng.zhang@ucf.edu) (Teng Zhang)

recovery (RSR), where the goal is to identify a low-dimensional subspace that explains a subset of the data points (inliers) while ignoring the effect of corrupted data (outliers). Unlike classical PCA, which assumes Gaussian-distributed noise, RSR explicitly models the data as a mixture of inliers that lie near or on a low-dimensional subspace and outliers that may be arbitrarily positioned.

Formally, we consider a dataset of  $n$  observations in  $\mathbb{R}^D$ , denoted by the multiset  $\mathcal{X}$ . This multiset consists of an inlier multiset and an outlier multiset,  $\mathcal{X} = \mathcal{X}_{\text{in}} \cup \mathcal{X}_{\text{out}}$ , where the inliers lie on a  $d$ -dimensional subspace  $L_*$ . For clarity, we focus on the noiseless inlier setting in this paper. The RSR problem seeks to recover  $L_*$  given only  $\mathcal{X}$ .

In the following, we focus on global convergence. That is, we say that an iterative algorithm *globally recovers* a point if it converges to that point from any initialization. To accomplish this, we revisit the IRLS method for RSR from Lerman and Maunu (2018a), known as the Fast Median Subspace (FMS) algorithm. FMS seeks to minimize a robust, nonconvex, least absolute deviations energy function over the Grassmannian manifold  $\mathcal{G}(D, d)$ , which is the set of  $d$ -dimensional linear subspaces in  $\mathbb{R}^D$ .

The focus of this paper is efficient solutions to the RSR problem when the subspace  $L_*$  and the dataset  $\mathcal{X}$  satisfies certain conditions. We say that a subspace  $L$  and dataset  $\mathcal{X}$  satisfy *deterministic conditions* if there exist nonrandom functions  $g_i$  such that  $g_i(\mathcal{X}_{\text{in}}, \mathcal{X}_{\text{out}}, L) \geq 0$ ,  $i = 1, \dots, k$ . These functions encode conditions that compare the statistics of the inliers and outliers, and we formulate our specific conditions later in Section 4.1. At a high level, such conditions end up being sufficient for solving the RSR problem efficiently, while in general it is NP-hard Clarkson and Woodruff (2015).

The rest of this section is organized as follows: Section 1.1 presents the primary contributions of our work. Then, Section 1.2 discusses the organization of the paper, and Section 1.3 introduces the necessary notation.

### 1.1. Contributions

The goals of our work are threefold: (i) to develop strong theoretical guarantees for FMS, (ii) to generalize these guarantees to affine subspaces, and (iii) to provide further practical motivation for FMS. We have made significant progress in all three directions. In particular, our key contributions are:

1. Under deterministic conditions on  $\mathcal{X}$  alone, FMS with a dynamically decreasing smoothing linearly converges to  $L_*$  from arbitrary initialization. To the best of our knowledge, this is the first global convergence result for IRLS on a Riemannian manifold in a nonconvex setting.
2. Under the same deterministic conditions on  $\mathcal{X}$  alone, the FMS algorithm with fixed regularization converges to a point close to  $L_*$  from arbitrary initialization.

3. We extend FMS to the estimation of affine subspaces. For this new algorithm, we establish local linear convergence under a modified set of deterministic conditions on  $\mathcal{X}$  and the initialization.
4. We run numerical experiments that demonstrate the advantages of dynamic smoothing for robust subspace recovery in adversarial settings.
5. We demonstrate the practical utility of FMS through an application to low-dimensional neural network training.

These results address a long-standing question of establishing broader theoretical guarantees that align with the empirical performance of FMS while also introducing new applications in modern machine learning. These results should also be of broad interest to the machine learning community. In particular, IRLS is a specific instance of a more general paradigm in optimization known as *Majorize-Minimization algorithms*. These algorithms are based on upper bounding a complex objective function with a function whose minimum is simpler to compute. One can generate a sequence that monotonically decreases the objective value by iteratively minimizing this upper bound. These algorithms have been widely used in signal processing and machine learning (Wiesel and Zhang, 2015; Sun et al., 2016), and can help understand machine learning building blocks like transformers (Yang et al., 2022).

Furthermore, our algorithms are specific instances of *Riemannian optimization algorithms*, which operate when the constraint set is a Riemannian manifold. There has been broad interest in studying properties of these methods (Absil et al., 2007; Boumal, 2023) and their practical application, for examples, see Vandereycken (2013); Jaquier et al. (2020); Hu et al. (2020).

Finally, there has also been widespread interest in analyzing the convergence of nonconvex optimization algorithms, which is notoriously difficult (Danilova et al., 2022). Fortunately, in many settings, nonconvex problems exhibit benign properties (Li et al., 2019) that enable favorable algorithmic behavior (Maunu et al., 2019). Most past results rely on gradient-based optimization, and this work complements them by providing a global convergence result for a nonconvex IRLS algorithm on a Riemannian manifold under a deterministic condition.

## 1.2. Paper Organization

In Section 2, we rigorously define the robust subspace recovery problem, provide the necessary mathematical background, and review related work. In Section 3, we propose our dynamic smoothing scheme in the FMS algorithm and its variant for estimating affine subspaces. In Section 4, we establish the theoretical guarantees for the proposed method. In Section 5, we run simulations on synthetic data that demonstrate the competitiveness of FMS with dynamic smoothing, and we also present the effective application of FMS in dimension-reduced training of neural networks.

### 1.3. Notation

For a finite multiset  $\mathcal{X}$ ,  $|\mathcal{X}|$  denotes the number of points. We use bold uppercase letters for matrices and bold lowercase letters for column vectors. Let  $\mathbf{I}_k$  denote the identity matrix in  $\mathbb{R}^{k \times k}$ , where if  $k$  is obvious, we simply write  $\mathbf{I}$ . For  $d \leq D$ ,  $\mathcal{O}(D, d)$  is the set of semi-orthogonal matrices in  $\mathbb{R}^{D \times d}$ , i.e.,  $\mathbf{U} \in \mathcal{O}(D, d)$  if and only if  $\mathbf{U}^T \mathbf{U} = \mathbf{I}_d$ . For a  $d$ -dimensional linear subspace  $L$ , we denote by  $\mathbf{P}_L$  the  $D \times D$  matrix representing the orthogonal projector onto  $L$ , and  $\mathbf{Q}_L = \mathbf{P}_{L^\perp}$  the projection onto the orthogonal complement of  $L$ . Projection matrices are symmetric and satisfy  $\mathbf{P}_L^2 = \mathbf{P}_L$  and  $\text{im}(\mathbf{P}_L) = L$ , where  $\text{im}(\cdot)$  denotes the column space of a matrix. For a matrix  $\mathbf{A}$ ,  $\|\mathbf{A}\|_2$  denotes its operator or spectral norm, and  $\|\mathbf{A}\|_F$  denotes its Frobenius norm. Further,  $\sigma_j(\mathbf{A})$  will denote the  $j$ th singular value of  $\mathbf{A}$ . For our inlier-outlier dataset  $\mathcal{X}$ , we let  $n = |\mathcal{X}|$ ,  $n_{\text{in}} = |\mathcal{X}_{\text{in}}|$ , and  $n_{\text{out}} = |\mathcal{X}_{\text{out}}|$ .

## 2. Problem Setup and Related Work

This section sets the stage for our algorithm and our theoretical results. In Section 2.1, we rigorously define the problem we seek to solve and provide the necessary mathematical background. After this, we review related work in Section 2.2.

### 2.1. Problem Formulation and Background

We briefly summarize the necessary background to understand the primary contributions of this work, building upon the setup provided in the introduction. For simplicity, we formulate the problem for linear subspaces. The treatment of affine subspaces is discussed in Section 3.2.

Let  $\text{dist}(\mathbf{x}, L) = \|\mathbf{Q}_L \mathbf{x}\|$  be the orthogonal distance between  $\mathbf{x} \in \mathcal{X}$  and  $L \in \mathcal{G}(D, d)$ , where  $\mathbf{Q}_L$  is the orthogonal projection onto the orthogonal complement of  $L$ . This paper investigates an IRLS approach to a nonconvex least absolute deviations formulation for RSR (Ding et al., 2006; Zhang et al., 2009; Maunu et al., 2019). This formulation minimizes the sum of distances from the data points to any  $d$ -dimensional subspace in  $\mathcal{G}(D, d)$ :

$$\hat{L} = \arg \min_{L \in \mathcal{G}(D, d)} F(L) := \sum_{\mathbf{x} \in \mathcal{X}} \text{dist}(\mathbf{x}, L), \quad (1)$$

This is an optimization problem over the Grassmannian manifold (Edelman et al., 1998). In fact, if we minimize the sum of squared distances  $\sum_{\mathbf{x} \in \mathcal{X}} \text{dist}^2(\mathbf{x}, L)$ , then we obtain the principal subspace. By using the non-squared distance instead, our estimator is less prone to the impact of large outliers.

An IRLS method for (1) iteratively applies weighted PCA. More specifically, at iteration  $k$  its unregularized version minimizes  $\sum_{\mathbf{x} \in \mathcal{X}} w_{\mathbf{x}} \text{dist}^2(\mathbf{x}, L)$  with weights  $w_{\mathbf{x}} = 1/\text{dist}(\mathbf{x}, L_{k-1})$  to find the updated subspace  $L_k$ . Here,  $L_k$  is the subspace estimated in the previous iteration. While this

method is elegant and widely used, it lacks global convergence and exact recovery guarantees, and this paper aims to fill this gap. Nevertheless, our theoretical analysis requires some modification of this simple procedure (see discussion of dynamic smoothing in Section 3). This analysis advances the state of nonconvex IRLS for Riemannian manifolds, specifically the Grassmannian  $\mathcal{G}(D, d)$ . Furthermore, it is natural to extend (1) by replacing  $\mathcal{G}(D, d)$  with the set of affine subspaces. This is the subject of our algorithmic development in Section 3.2.

The analysis in this paper depends on the principal angles and vectors between subspaces as follows: For any  $L_0, L_1 \in \mathcal{G}(D, d)$ , we denote their  $d$  principal angles by  $\{\theta_j(L_0, L_1)\}_{j=1}^d$  and let the respective principal vectors for  $L_0$  and  $L_1$  be  $\{\mathbf{u}_j(L_0, L_1)\}_{j=1}^d$  and  $\{\mathbf{v}_j(L_0, L_1)\}_{j=1}^d$ . Given bases  $\mathbf{W}_0 \in \mathcal{O}(D, d)$  for  $L_0$  and  $\mathbf{W}_1 \in \mathcal{O}(D, d)$  for  $L_1$ , one can compute the principal vectors and angles by the singular value decomposition  $\mathbf{W}_0^T \mathbf{W}_1 = \mathbf{R}_0 \cos(\mathbf{\Theta}) \mathbf{R}_1^T$ , in which case  $\mathbf{\Theta}$  contains the principal angles,  $\mathbf{W}_0 \mathbf{R}_0$  contains the vectors  $\mathbf{u}_j$  and  $\mathbf{W}_1 \mathbf{R}_1$  contains the vectors  $\mathbf{v}_j$ . See Lerman and Zhang (2014, Section 3.2.1) for a more detailed treatment.

## 2.2. Review of Related Work

In the following, we separately discuss related work in robust subspace recovery, iterative reweighted least squares, and the least absolute deviations-based RSR problem (1).

### 2.2.1. Robust Subspace Recovery (RSR)

RSR has been extensively studied in various contexts, with methods falling into several key categories. For a comprehensive review, see Lerman and Maunu (2018b). The distinction between our problem and robust PCA (RPCA) (Candès et al., 2011) should be noted. While both deal with corrupted low-rank structures, RPCA assumes elementwise corruptions throughout the data matrix, whereas RSR assumes some samples are wholly corrupted. Consequently, algorithms designed for one problem typically do not perform well on the other.

A significant direction involves robust covariance estimation. Methods like Tyler’s M-estimator (TME) (Tyler, 1987; Zhang, 2016) aim to robustly estimate an underlying covariance matrix from which the principal subspace can be extracted. These approaches have strong theoretical foundations regarding breakdown points, though their guarantees for subspace recovery are more limited in natural special settings. Stronger local guarantees were obtained for a subspace-constrained TME variant (Yu et al., 2024; Lerman et al., 2024).

Many approaches frame RSR as an outlier filtering problem, where the goal is first identifying and removing outliers before applying standard PCA. Examples include RANSAC-based methods (Fischler and Bolles, 1981; Arias-Castro and Wang, 2017; Maunu and Lerman, 2019) and more recent approaches like coherence pursuit (Rahmani and Atia, 2017). While conceptually simple, these

methods often require careful parameter tuning and may struggle with high outlier percentages and higher intrinsic subspace dimensions.

### 2.2.2. *Least Absolute Deviations-based RSR*

In this work, we focus on a specific approach to solving the RSR problem that relies on *least absolute deviations*, i.e., the objective function in (1). This has been a focus of a major line of work, where one replaces the squared Euclidean distance in PCA with the absolute distance to achieve robustness. While this problem is computationally hard (Hardt and Moitra, 2013; Clarkson and Woodruff, 2015), several methods have been proposed to approximately solve it. These include convex relaxations like Outlier Pursuit (Xu et al., 2012) and REAPER (Lerman et al., 2015), as well as nonconvex approaches like geodesic gradient descent (Maunu et al., 2019), which can be easily replaced with projected subgradient descent (PSGM) (Zhu et al., 2018). The problem may also be addressed using Riemannian ADMM (Li et al., 2024), a general framework for manifold optimization with nonsmooth objectives. In addition, PSGM and manifold proximal point algorithm (Chen et al., 2019) have also been proposed for Dual Principal Component Pursuit (DPCP), which can be considered as a special case of (1), where  $d$  is replaced by  $D - d$  (Zhu et al., 2018). Indeed, the analysis of these methods is analogous to that of Maunu et al. (2019). We remark that the analysis pursued in Zhu et al. (2018) only holds for the special case  $d = D - 1$ . It was later generalized for any  $d$  in Ding et al. (2021), again with similar ideas to Maunu et al. (2019), whose result holds for any subspace dimension.

This work investigates the FMS method proposed by Lerman and Maunu (2018a), which solves (1) using IRLS. This method is popular due to its simplicity and strong empirical performance. More recently, FMS has also been applied to hierarchical representations (Ding et al., 2024).

However, the theoretical analysis of the FMS algorithm is somewhat limited, as it generally guarantees convergence only to stationary points. In contrast, Maunu et al. (2019) investigates the landscape of the objective function and obtains a theoretical understanding of its associated gradient descent algorithm. However, they only use this analysis to prove local convergence of gradient descent, which requires significant parameter tuning. Also, until now, it has been unclear how this analysis can extend to other optimization frameworks like IRLS, which we will discuss next.

### 2.2.3. *Iteratively Reweighted Least Squares (IRLS)*

The method of IRLS is used to solve specific optimization problems with objective functions that are sums of loss functions applied to residuals (Holland and Welsch, 1977). In each step the method solves a weighted least squares problem.

This idea has been applied in numerous problems, such as geometric median (Weiszfeld, 1937; Kuhn, 1973), robust regression (Holland and Welsch, 1977; Peng et al., 2024), M-estimator in robust statistics (Maronna et al., 2006),  $\ell_q$  norm-based sparse recovery (Daubechies et al., 2010; Kümmerle et al., 2020), low-rank matrix recovery (Fornasier et al., 2011), synchronization (Chatterjee and Govindu, 2017), and more. In particular, IRLS algorithms have also been used to solve the convex relaxation of (1) in Zhang and Lerman (2014); Lerman et al. (2015).

Despite their strong empirical performance, straightforward IRLS algorithms generally lack strong theoretical guarantees. To illustrate this, for the geometric median problem (Weiszfeld, 1937; Beck and Sabach, 2015), which minimizes  $F(\mathbf{x}) = \sum_{i=1}^n \|\mathbf{x} - \mathbf{x}_i\|$ , an IRLS method iteratively reweights the data points with weights  $w_i^{(k)} = 1/\|\mathbf{x}^{(k)} - \mathbf{x}_i\|$ . If  $\mathbf{x}^{(k)} = \mathbf{x}_1$ , then  $\mathbf{x}^{(k+1)} = \mathbf{x}_1$ , as the weight for  $\mathbf{x}_1$  becomes infinite. Daubechies et al. (2010) indicate the same problem of infinite weight in IRLS for sparse recovery. To address this issue, a common strategy is to introduce a smoothing parameter that bounds the weights from above, like choosing  $w_i^{(k)} = 1/(\epsilon^2 + \|\mathbf{x}_i - \mathbf{x}\|^2)^{1/2}$  or  $w_i = 1/\max(\epsilon, \|\mathbf{x}_i - \mathbf{x}\|)$ . This strategy is used heuristically in Zhang and Lerman (2014); Lerman et al. (2015). Still, as pointed out in Peng et al. (2024), this method only converges to an  $\epsilon$ -approximate solution, and no theory exists on its global convergence rate.

Researchers have used different insights to reach a consensus on dynamically updating the weights (Daubechies et al., 2010; Fornasier et al., 2011). Recent advances in IRLS (Kümmerle et al., 2020; Peng et al., 2024) suggest applying the “Dynamic Smoothing Parameter” strategy, which adaptively chooses the regularization parameter based on the current weights. Under this strategy, they prove that the IRLS algorithm converges linearly to the solution of the original problem. However, we note that such an analysis of IRLS has not been applied to manifold optimization problems such as RSR, and the only theoretical guarantee in nonconvex optimization provided in Peng et al. (2024) yields a local result in which the initialization must be very close to the solution.

Another work that examines dynamic smoothing on manifolds is Beck and Rosset (2023), where the authors prove a sublinear convergence rate for a gradient method to a stationary point.

### 3. FMS: Review and Extension to Affine Subspaces

In this section, we outline our algorithmic contributions to the RSR problem. In Section 3.1, we review the FMS algorithm and discuss the addition of dynamic smoothing. Then, in Section 3.2, we discuss a novel affine variant of the FMS algorithm.

### 3.1. The FMS Algorithm

Here, we study the iteratively reweighted least-squares method (IRLS) to solve (1), which alternates between finding the top eigenvectors of a weighted covariance and updating the weights. We recall that the unregularized IRLS method at the  $k$ -th iteration is the solution to the weighted squared problem of

$$L^{(k+1)} = \arg \min_L \sum_{\mathbf{x} \in \mathcal{X}} w_{\mathbf{x}}^{(k)} \text{dist}(\mathbf{x}, L)^2, \text{ where } w_{\mathbf{x}}^{(k)} = \frac{1}{\text{dist}(\mathbf{x}, L^{(k)})}. \quad (2)$$

This solution coincides with the standard PCA procedure:

$$L^{(k+1)} = T(L^{(k)}) = \text{span of top } d \text{ eigenvectors of } \sum_{\mathbf{x} \in \mathcal{X}} w_{\mathbf{x}}^{(k)} \mathbf{x} \mathbf{x}^T. \quad (3)$$

To put forward an IRLS algorithm that gives a re-weighting without infinite components in the weight, it is natural to regularize the weights to be  $w_{\mathbf{x}}^{(k)} = 1/\max(\text{dist}(\mathbf{x}, L^{(k)}), \epsilon_k)$ . The FMS algorithm by Maunu et al. (2019) adopts a fixed regularization  $\epsilon_k$  for all  $k \geq 0$ .

In this work, we propose to choose  $\epsilon_k$  in each step adaptively by incorporating a ‘‘Dynamic Smoothing Parameter’’ procedure

$$\epsilon_k = \min(\epsilon_{k-1}, q_{\gamma}(\{\text{dist}(\mathbf{x}, L^{(k)})\}_{\mathbf{x} \in \mathcal{X}})), \quad (4)$$

where  $q_{\gamma}$  represents the  $\gamma$ -th quantile. This is defined as

$$q_{\gamma}(\{\text{dist}(\mathbf{x}, L^{(k)})\}_{\mathbf{x} \in \mathcal{X}}) = \max \left\{ a \in \mathbb{R} : \frac{|\{\mathbf{x} \in \mathcal{X} : \text{dist}(\mathbf{x}, L^{(k)}) \leq a\}|}{|\mathcal{X}|} \leq \gamma \right\}$$

One can think of  $\gamma$  as an inlier-percentage hyperparameter. This choice is inspired from Kümmerle et al. (2020); Peng et al. (2024), and ensures that  $\epsilon_k$  forms a nonincreasing sequence while remaining sufficiently large relative to the set  $\{\text{dist}(\mathbf{x}, L^{(k)})\}_{\mathbf{x} \in \mathcal{X}}$ . We summarize the regularized IRLS in Algorithm 1, which we refer to as Fast Median Subspace with Dynamic Smoothing (FMS-DS).

Dynamic smoothing allows for the parameter  $\epsilon$  to converge to zero along the iterations. This leads to a procedure that can recover a solution to the unregularized problem by solving a sequence of regularized problems. This is made rigorous in Section 4.

The FMS-DS algorithm requires three inputs: an initial guess at the subspace  $L^{(0)}$ , a lower bound on the percentage of inliers  $\gamma$ , and an initial regularization hyperparameter  $\epsilon_{-1}$ . The parameters  $\gamma$  and  $\epsilon_{-1}$  can be estimated using prior knowledge or cross-validation.

### 3.2. The Affine FMS Algorithm

Most existing works on RSR (see Section 2.2) focus on recovering a robust linear  $d$ -dimensional subspace in  $\mathbb{R}^D$ . While our main theoretical results concern this linear case, our objective function (1)



---

**Algorithm 1** FMS-DS

---

**Input:** Set of observations  $\mathcal{X} \subset \mathbb{R}^D$ , initial estimated subspace  $L^{(0)} \subset \mathcal{G}(D, d)$ ,  $\gamma$ : inlier percentage hyperparameter, initial regularization hyperparameter  $\epsilon_{-1}$

**Output:** An estimate of the underlying subspace.

**Steps:**

**1:** Let  $k = 0$ .

**2:** Choose  $\epsilon_k$  suitably from  $L^{(k)}$  and  $\mathcal{X}$  by (4).

**3:**  $L^{(k+1)} = T_{\epsilon_k}(L^{(k)})$ , where

$$T_{\epsilon}(L) = \text{span of top } d \text{ eigenvectors of } \sum_{i=1}^n \frac{\mathbf{x}_i \mathbf{x}_i^T}{\max(\text{dist}(\mathbf{x}_i, L), \epsilon)}. \quad (5)$$

**4:**  $k = k + 1$ .

**5:** Repeat Steps 2-4 until convergence.

---

and its IRLS algorithm naturally extend to the affine setting, allowing for robust local recovery of an affine  $d$ -dimensional subspace.

Here we use  $\mathcal{A}(D, d)$  to denote the set of all  $d$ -dimensional affine subspaces in  $\mathbb{R}^D$ . We distinguish between a representative pair  $A = (L, \mathbf{m}) \in \mathcal{G}(D, d) \times \mathbb{R}^D$ , and the affine subspace  $[A] = \{\mathbf{m} + \mathbf{x} : \mathbf{x} \in L\}$ , which is the affine subspace formed by translating the  $d$ -dimensional linear subspace  $L$  by  $\mathbf{m}$ . The representative pair is not unique, since  $(L, \mathbf{m})$  and  $(L, \mathbf{m}')$  refer to the same affine subspace whenever  $\mathbf{m}' = \mathbf{m} + \mathbf{P}_L \boldsymbol{\delta}$  for some  $\boldsymbol{\delta} \in \mathbb{R}^D$ . In fact,  $[A]$  is an equivalence class of representative pairs. For any  $\mathbf{x} \in \mathbb{R}^D$ , the distance to  $[A]$  is given by  $\text{dist}(\mathbf{x}, [A]) = \|\mathbf{Q}_L(\mathbf{x} - \mathbf{m})\|$ , which is invariant under the choice of representative.

We consider the following natural generalization of (1):

$$[\hat{A}] = \arg \min_{[A] \in \mathcal{A}(D, d)} F^{(a)}([A]) := \sum_{\mathbf{x} \in \mathcal{X}} \text{dist}(\mathbf{x}, [A]) = \sum_{\mathbf{x} \in \mathcal{X}} \|\mathbf{Q}_L(\mathbf{x} - \mathbf{m})\|. \quad (6)$$

This problem is invariant to the choice of representation, and so we rewrite it in parametrized form as

$$\hat{A} = \arg \min_{A \in \mathcal{G}(D, d) \times \mathbb{R}^D} F^{(a)}(A) := \sum_{\mathbf{x} \in \mathcal{X}} \text{dist}(\mathbf{x}, A) = \sum_{\mathbf{x} \in \mathcal{X}} \|\mathbf{Q}_L(\mathbf{x} - \mathbf{m})\|. \quad (7)$$

To solve this problem, we generalize Algorithm 1 based on a straightforward generalization of the argument in Section 3.1. The affine IRLS method iterates by solving the weighted least squares problem at the  $k$ th iteration, where we replace distances to linear subspaces with distances to affine

subspaces. The affine setting of the FMS algorithm can thus be written as

$$A^{(k+1)} = T_{\epsilon_k}^{(a)}(A^{(k)}) := \arg \min_{A \in \mathcal{A}(D, d)} \sum_{\mathbf{x} \in \mathcal{X}} w_{\mathbf{x}}^{(k)} \text{dist}(\mathbf{x}, A)^2, \text{ where } w_{\mathbf{x}}^{(k)} = \frac{1}{\max(\text{dist}(\mathbf{x}, A^{(k)}), \epsilon_k)}. \quad (8)$$

The solution can be obtained from the standard PCA procedure applied to  $\mathbf{x} \in \mathcal{X}$  with weights  $1/\text{dist}(\mathbf{x}, A^{(k)})$ . Therefore,  $T_{\epsilon}^{(a)}(A) = (L, \mathbf{m})$  is such that  $\mathbf{m} = \sum_{\mathbf{x} \in \mathcal{X}} w_{\mathbf{x}} \mathbf{x} / \sum_{\mathbf{x} \in \mathcal{X}} w_{\mathbf{x}}$ , where  $w_{\mathbf{x}} = 1/\max(\text{dist}(\mathbf{x}, A), \epsilon)$ , and  $L$  is the span of top  $d$  eigenvectors of  $\sum_{\mathbf{x} \in \mathcal{X}} w_{\mathbf{x}}(\mathbf{x} - \mathbf{m})(\mathbf{x} - \mathbf{m})$ .

Similar to the linear case in (4), we choose the regularization parameters using dynamic smoothing. In this case, the update for  $\epsilon$  becomes

$$\epsilon_k = \min(\epsilon_{k-1}, q_{\gamma}(\{\text{dist}(\mathbf{x}, A^{(k)})\}_{\mathbf{x} \in \mathcal{X}})). \quad (9)$$

Again,  $\gamma$  is an inlier-percentage hyperparameter. We refer to the resulting algorithm as Affine Fast Median Subspace with Dynamic Smoothing (AFMS-DS). The method with fixed regularization is just referred to as Affine FMS (AFMS).

**Remark 1.** *AFMS is rotation and translation equivariant, in the sense that if  $T_{\epsilon}^{(a)}(A) = (L, \mathbf{m})$ , then  $T_{\epsilon}^{(a)}(\mathbf{R}A + \mathbf{a}) = (\mathbf{R}L, \mathbf{R}\mathbf{m} + \mathbf{a})$  for any  $\mathbf{R}^T \mathbf{R} = \mathbf{I}_D$  and  $\mathbf{a} \in \mathbb{R}^D$ . Furthermore, FMS is a special case of AFMS with the mean parameter fixed to be zero.*

#### 4. Theoretical Analysis

This section establishes theoretical guarantees for the (A)FMS-DS algorithms by showing that the algorithms recover an underlying linear or affine subspace under specific inlier-outlier models. We emphasize that, in the case of FMS-DS, we achieve a global result, namely, the algorithm converges to the underlying subspace from any initialization. The main theorem for FMS-DS is presented in Section 4.1, with further discussion of this result presented in Sections 4.1.1 and 4.1.2. We then establish a local convergence theorem for AFMS-DS in Section 4.2.

##### 4.1. Main Result for Linear Subspace Recovery

This section establishes a linear convergence guarantee for Algorithm 1. The main result, Theorem 1 shows that the algorithm linearly converges to an underlying subspace from any initialization if certain conditions on the data are satisfied.

To state our theorem, we first define a regularized objective  $F_{\epsilon}(L)$ :

$$F_{\epsilon}(L) = \sum_{\mathbf{x} \in \mathcal{X}: \text{dist}(\mathbf{x}, L) > \epsilon} \text{dist}(\mathbf{x}, L) + \sum_{\mathbf{x} \in \mathcal{X}: \text{dist}(\mathbf{x}, L) \leq \epsilon} \left( \frac{1}{2} \epsilon + \frac{\text{dist}(\mathbf{x}, L)^2}{2\epsilon} \right). \quad (10)$$

This is a natural extension of (1) as we view it as the objective function for IRLS with a fixed regularization parameter (Zhang and Lerman, 2014; Lerman et al., 2015; Daubechies et al., 2010; Kümmerle et al., 2020; Peng et al., 2024).

Next, we introduce the two assumptions needed for our main theorem. Both of these assumptions are restrictions on the inlier-outlier dataset  $\mathcal{X}$ . The first assumption requires that low-dimensional subspaces that are not  $L_\star$  may not contain a significant number of points.

**Assumption 1.** *Let  $\gamma_\star = |\mathcal{X}_{\text{in}}|/|\mathcal{X}|$  be the percentage of inliers and  $\gamma$  the inlier-percentage hyperparameter for FMS-DS. For all  $d-1$ -dimensional linear subspaces  $L_0 \subset L_\star$  and  $d$ -dimensional linear subspaces  $L \neq L_\star$ ,  $|\mathcal{X} \cap (L_0 \cup L)|/|\mathcal{X}| < \gamma < \gamma_\star/2$ .*

**Remark 2.** *Assumption 1 can be weakened to instead assume that  $L = L_\star$  is the unique subspace such that  $q_\gamma(\{\mathbf{x}, L\}_{\mathbf{x} \in \mathcal{X}}) = 0$ . However, in this case, we can only establish convergence to  $L_\star$ , and we lose the linear convergence rate guarantee.*

The second assumption requires the definition of two summary statistics  $S_{\text{in}}$  and  $S_{\text{out}}$ .

$$S_{\text{in}} = \min_{\mathbf{u} \in L_\star: \|\mathbf{u}\|=1} \sum_{\mathbf{x} \in \mathcal{X}_{\text{in}}} |\mathbf{u}^T \mathbf{x}|, \quad S_{\text{out}} = \max_{L \in \mathcal{G}(D, d)} \left\| \sum_{\mathbf{x} \in \mathcal{X}_{\text{out}}} \frac{\mathbf{P}_L \mathbf{x} \mathbf{x}^T \mathbf{P}_{L^\perp}}{\text{dist}(\mathbf{x}, L)} \right\|_2. \quad (11)$$

Heuristically, the statistic  $S_{\text{in}}$  measures how well-spread the inliers are on the underlying subspace, while the statistic  $S_{\text{out}}$  shows how well-aligned the outliers are along any  $d$ -dimensional subspace. Both statistics are somewhat natural. A large  $S_{\text{in}}$  prevents inliers from lying on or close to low-dimensional subspaces of  $L_\star$ . The statistic  $S_{\text{in}}$  is zero when there is a direction in  $L_\star$  that is orthogonal to all inliers, and it is large when every direction in  $L_\star$  has many inliers significantly correlated with it. On the other hand, having a small  $S_{\text{out}}$  is also natural, since it prevents outliers from being too low-dimensional. We remark that the  $S_{\text{in}}$  statistic is the same as the permeance statistic in Lerman et al. (2015), and the  $S_{\text{out}}$  statistic is the alignment statistic of Maunu et al. (2019).

In line with the discussion in the previous paragraph, the second assumption ensures that the inlier statistic  $S_{\text{in}}$  is sufficiently larger than  $S_{\text{out}}$ . This holds in a wide variety of cases, see the discussions in Maunu et al. (2019); Maunu and Lerman (2019) as well as Section 4.1.1.

**Assumption 2.** *For the inlier-outlier dataset  $\mathcal{X}$ , there exists a  $\theta_0 \in [0, \pi/2]$  and an  $\epsilon_{-1}$  such that for all  $\epsilon \leq \epsilon_{-1}$ , the following deterministic conditions are satisfied:*

$$\frac{S_{\text{out}}}{\sigma_d(\sum_{\mathbf{x} \in \mathcal{X}_{\text{in}}} \mathbf{x} \mathbf{x}^T / \max(\|\mathbf{x}\|, \epsilon))} \leq \sin \theta_0, \quad \cos \theta_0 S_{\text{in}} \geq \sqrt{d} S_{\text{out}}. \quad (12)$$

With these assumptions, we are now ready to present our main theorem. This theorem guarantees the global convergence of FMS-DS with a linear rate.

**Theorem 1.** *[Global Linear Convergence of FMS-DS] Let  $\mathcal{X}$  be a dataset satisfying Assumptions 1 and 2 for given constants  $\gamma, \epsilon_{-1} > 0$ . Then, the sequence  $L^{(k)}$  generated by Algorithm 1 with initial dynamic smoothing parameter  $\epsilon_{-1}$  and inlier percentage hyperparameter  $\gamma$  converges to  $L_\star$  in the sense that  $\lim_{k \rightarrow \infty} \|\mathbf{P}_{L^{(k)}} - \mathbf{P}_{L_\star}\|_2 \rightarrow 0$ . In addition, the sequence  $F_{\epsilon_k}(L^{(k)})$  is nonincreasing and there exists a  $0 < c < 1$  such that*

$$F(L^{(k)}) - F(L_\star) \leq c^k (F(L^{(0)}) - F(L_\star)).$$

To prove Theorem 1, we rely on several lemmas. To improve readability, the proof of these lemmas is deferred to Section 6.1.

*Proof of Theorem 1.* We begin the proof with two lemmas. The first lemma is a simple monotonicity property on the regularized objective function  $F_\epsilon$  defined in (10).

**Lemma 1** (Properties of smoothed objective function). *For any  $\epsilon_1 < \epsilon_2$ ,  $F_{\epsilon_1}(L) \leq F_{\epsilon_2}(L)$ . In addition,  $F_0(L) = F(L)$ .*

The second lemma shows that the smoothed objective value is nonincreasing over iterations of Algorithm 1, where the amount of decrease is quantified.

**Lemma 2** (Decrease over iterations). *For all  $k \geq 1$ , we have*

$$F_{\epsilon_k}(L^{(k)}) - F_{\epsilon_k}(L^{(k+1)}) \geq \frac{\|\mathbf{P}_{L^{(k)}} \mathbf{S}_{L^{(k)}, \epsilon_k} \mathbf{Q}_{L^{(k)}}\|_F^2}{2\|\mathbf{S}_{L^{(k)}, \epsilon_k}\|}, \quad (13)$$

where

$$\mathbf{S}_{L, \epsilon} = \sum_{\mathbf{x} \in \mathcal{X}} \frac{\mathbf{x} \mathbf{x}^T}{\max(\epsilon, \text{dist}(\mathbf{x}, L))}. \quad (14)$$

Using the fact that  $\epsilon_k$  is nonincreasing, Lemmas 1 and 2 imply that the sequence  $F_{\epsilon_k}(L^{(k)})$  are nonincreasing:

$$F_{\epsilon_k}(L^{(k)}) - F_{\epsilon_{k+1}}(L^{(k+1)}) \geq F_{\epsilon_k}(L^{(k)}) - F_{\epsilon_k}(L^{(k+1)}) \geq 0. \quad (15)$$

As a result, by basic monotonic convergence theory, the sequence  $F_{\epsilon_k}(L^{(k)})$  must converge.

The third lemma establishes a lower bound on the decrease  $F_{\epsilon_k}(L^{(k)}) - F_{\epsilon_k}(L^{(k+1)})$ , and write it in terms of the statistics  $S_{\text{in}}$  and  $S_{\text{out}}$ . This allows us to go from convergence of objective values to convergence of the iterates themselves.

**Lemma 3** (Nonzero gradient, local guarantee). *If  $\epsilon$  is chosen such that for at least half of the inliers,  $\text{dist}(\mathbf{x}, L) > \epsilon$ , that is,  $|\{\mathbf{x} \in \mathcal{X}_{\text{in}} : \text{dist}(\mathbf{x}, L) > \epsilon\}| \geq \frac{1}{2}|\mathcal{X}_{\text{in}}|$ , then*

$$\|\mathbf{P}_L \mathbf{S}_{L, \epsilon} \mathbf{Q}_L\|_F \geq \frac{\cos \theta_1(L, L_\star)}{2\sqrt{d}} S_{\text{in}} - S_{\text{out}}, \quad \|\mathbf{S}_{L, \epsilon}\| \leq \frac{\|\mathbf{X}\|^2}{\epsilon}.$$

Combining (15), Lemma 2, and Lemma 3, we have

$$F_{\epsilon_k}(L^{(k)}) - F_{\epsilon_{k+1}}(L^{(k+1)}) \geq \frac{\|\mathbf{P}_{L^{(k)}} \mathbf{S}_{L^{(k)}, \epsilon_k} \mathbf{P}_{L^{(k)} \perp}\|_F}{2\|\mathbf{S}_{L^{(k)}, \epsilon_k}\|} \geq \epsilon_k \frac{S_{\text{in}} \cos \theta_0 - S_{\text{out}}}{2\|\mathbf{X}\|^2}. \quad (16)$$

Since the sequence  $F_{\epsilon_k}(L^{(k)})$  is lower bounded and monotonic,  $F_{\epsilon_k}(L^{(k)}) - F_{\epsilon_{k+1}}(L^{(k+1)})$  converges to zero. Thus (16) implies that  $\epsilon_k$  converges to zero as well.

Algorithm 1 implies that there exists a subsequence  $1 \leq k_1 \leq k_2 \leq \dots$  such that  $\epsilon_{k_l} = q_\gamma(\{\text{dist}(\mathbf{x}, L^{(k_l)})\}_{\mathbf{x} \in \mathcal{X}})$ . Then  $\lim_{k \rightarrow \infty} \epsilon_k = 0$ . Since  $\epsilon_k \rightarrow 0$ , by Assumption 1,  $\text{dist}(\mathbf{x}, L^{(k_l)}) \rightarrow 0$  for all inliers  $\mathbf{x}$ . Since  $\text{dist}(\mathbf{x}, L)^2 = \sum_{j=1}^d \sin^2 \theta_j(L, L_\star) |\mathbf{x}^T \mathbf{u}_j(L, L_\star)|^2$ , this implies that all principal angles converge to zero, and as a result  $\mathbf{P}_{L^{(k)}} - \mathbf{P}_{L_\star}$  converges to zero.

We now proceed with the proof of linear convergence. To prove that  $F_{\epsilon_k}(L^{(k)})$  converges linearly, we will show that there exists  $C_0 > 0$  such that

$$F_{\epsilon_k}(L^{(k)}) - F(L_\star) < \epsilon_k C_0, \quad (17)$$

where

$$C_0 = \left( \left( 1 + \frac{\pi \sqrt{d} S_{\text{out}}}{2 S_{\text{in}}} \right) |\mathcal{X}_{\text{in}}|/c_3 + |\mathcal{X}|/2 \right),$$

and  $c_3$  is will be defined in Lemma 5. We note that this implies linear convergence because if (17) holds, then with (16) we have

$$F_{\epsilon_k}(L^{(k)}) - F_{\epsilon_{k+1}}(L^{(k+1)}) \geq \frac{\frac{S_{\text{in}} \cos \theta_0 - S_{\text{out}}}{2\|\mathbf{X}\|^2}}{C_0} (F_{\epsilon_k}(L^{(k)}) - F(L_\star)).$$

As a result,  $F_{\epsilon_k}(L^{(k)})$  converges linearly.

We establish (17) through our final two lemmas. The fourth lemma establishes a bound on the ratio of outlier and inlier objective values based on  $S_{\text{in}}$  and  $S_{\text{out}}$ .

**Lemma 4** (Bound on the objective value). *Let the inlier and outlier objectives be written as  $F_{\text{in}}(L) = \sum_{\mathbf{x} \in \mathcal{X}_{\text{in}}} \text{dist}(\mathbf{x}, L)$  and  $F_{\text{out}}(L) = \sum_{\mathbf{x} \in \mathcal{X}_{\text{out}}} \text{dist}(\mathbf{x}, L)$ . Denote the principal angles between  $L$  and  $L_\star$  by  $\theta_1, \dots, \theta_d$ , then*

$$\frac{|F_{\text{out}}(L) - F_{\text{out}}(L_\star)|}{F_{\text{in}}(L) - F_{\text{in}}(L_\star)} \leq \frac{\sqrt{d} S_{\text{out}} \sum_{j=1}^d \theta_j}{S_{\text{in}} \sum_{j=1}^d \sin \theta_j} \quad (18)$$

The fifth and final lemma establishes a connection between the quantiles of the set of distances and the inlier objective value that is useful for controlling the iterates  $\epsilon_k$ .

**Lemma 5.** *Under Assumption 1, there exists  $c_3 > 0$  such that for all  $L \in \mathcal{G}(D, d)$ ,*

$$q_\gamma(\{\text{dist}(\mathbf{x}, L)\}_{\mathbf{x} \in \mathcal{X}}) \geq c_3 \frac{F_{\text{in}}(L)}{|\mathcal{X}_{\text{in}}|}. \quad (19)$$

To prove (17), we begin with the natural bound

$$\begin{aligned}
F_{\epsilon_k}(L^{(k)}) &= \sum_{\mathbf{x} \in \mathcal{X}: \text{dist}(\mathbf{x}, L^{(k)}) > \epsilon_k} \text{dist}(\mathbf{x}, L^{(k)}) + \sum_{\mathbf{x} \in \mathcal{X}: \text{dist}(\mathbf{x}, L^{(k)}) \leq \epsilon_k} \left( \frac{1}{2} \epsilon_k + \frac{\text{dist}(\mathbf{x}, L^{(k)})^2}{2\epsilon_k} \right). \\
&\leq \sum_{\mathbf{x} \in \mathcal{X}} \text{dist}(\mathbf{x}, L^{(k)}) + \sum_{\mathbf{x} \in \mathcal{X}: \text{dist}(\mathbf{x}, L^{(k)}) \leq \epsilon_k} \epsilon_k \\
&\leq F(L^{(k)}) + \epsilon_k |\mathcal{X}|/2.
\end{aligned}$$

Second, Lemma 4 implies

$$\begin{aligned}
F(L^{(k)}) - F(L_\star) &= F_{\text{in}}(L^{(k)}) - F_{\text{in}}(L_\star) + F_{\text{out}}(L^{(k)}) - F_{\text{out}}(L_\star) \\
&\leq \left( 1 + \frac{S_{\text{out}} \sum_{j=1}^d \theta_j}{\frac{\sum_{j=1}^d \sin \theta_j}{\sqrt{d}} S_{\text{in}}} \right) (F_{\text{in}}(L^{(k)}) - F_{\text{in}}(L_\star))
\end{aligned}$$

Third, when  $\epsilon_k = q_\gamma(\{\text{dist}(\mathbf{x}, L^{(k)})\}_{\mathbf{x} \in \mathcal{X}})$ , Lemma 5 implies

$$(F_{\text{in}}(L^{(k)}) - F_{\text{in}}(L_\star)) = F_{\text{in}}(L^{(k)}) \leq |\mathcal{X}_{\text{in}}| \epsilon_k / c_3$$

Combining the three equations above,

$$\begin{aligned}
F_{\epsilon_k}(L^{(k)}) - F(L_\star) &\leq (F(L^{(k)}) - F(L_\star)) + \epsilon_k |\mathcal{X}|/2 \\
&\leq \left( 1 + \frac{S_{\text{out}} \sum_{j=1}^d \theta_j}{\frac{\sum_{j=1}^d \sin \theta_j}{\sqrt{d}} S_{\text{in}}} \right) (F_{\text{in}}(L^{(k)}) - F_{\text{in}}(L_\star)) + \epsilon_k |\mathcal{X}|/2 \\
&\leq \left( \left( 1 + \frac{S_{\text{out}} \sum_{j=1}^d \theta_j}{\frac{\sum_{j=1}^d \sin \theta_j}{\sqrt{d}} S_{\text{in}}} \right) |\mathcal{X}_{\text{in}}|/c_3 + |\mathcal{X}|/2 \right) \epsilon_k.
\end{aligned} \tag{20}$$

Using  $\theta \leq \frac{\pi}{2} \sin \theta$  for  $\theta \in [0, \pi/2]$ ,

$$\left( \left( 1 + \frac{S_{\text{out}} \sum_{j=1}^d \theta_j}{\frac{\sum_{j=1}^d \sin \theta_j}{\sqrt{d}} S_{\text{in}}} \right) |\mathcal{X}_{\text{in}}|/c_3 + |\mathcal{X}|/2 \right) \leq C_0$$

and (17) holds. When  $\epsilon_k \neq q_\gamma(\{\text{dist}(\mathbf{x}, L^{(k)})\}_{\mathbf{x} \in \mathcal{X}})$ , then there exists  $l < k$  such that  $\epsilon_k = \epsilon_l = q_\gamma(\{\text{dist}(\mathbf{x}, L^{(l)})\}_{\mathbf{x} \in \mathcal{X}})$  and we have

$$F_{\epsilon_k}(L^{(k)}) \leq F_{\epsilon_l}(L^{(l)}) \leq C_0 \epsilon_l = C_0 \epsilon_k,$$

where the second inequality follows from the argument of (20). □

We conclude with a few remarks.

**Remark 3** (Choice of  $c_3$  in Lemma 5). *By the proof of Lemma 5, it is sufficient to find  $c_3$  such that no more than  $\gamma/2\gamma_\star$  percentage of the inliers are in the set*

$$\{\mathbf{x} \in \mathcal{X}_{\text{in}} : |\mathbf{u}_1^T \mathbf{x}| \leq c_3 \text{mean}_{\mathbf{x} \in \mathcal{X}_{\text{in}}} \|\mathbf{x}\|\},$$

*for any  $\|\mathbf{u}_1\| = 1$ , where mean is the average value of the set, and no more than  $\gamma/2(1 - \gamma_\star)$  percentage of the outliers are contained in the region*

$$\{\mathbf{x} \in \mathcal{X}_{\text{out}} : |\mathbf{x}^T \mathbf{u}_2| \leq c_3 \text{mean}_{\mathbf{x} \in \mathcal{X}_{\text{in}}} \|\mathbf{x}\|\}$$

*for any  $\|\mathbf{u}_2\| = 1$ .*

**Remark 4.** *Compared to recent guarantees for IRLS (Daubechies et al., 2010; Kümmerle et al., 2020; Peng et al., 2024), our work represents a step forward in two key ways. We analyze an IRLS algorithm on a Riemannian manifold,  $\mathcal{G}(D, d)$ , and establish global convergence for a nonconvex problem, both of which are novel results in the literature. In contrast, most analyses rely on convex optimization, ensuring global convergence. The only work on IRLS with nonconvex  $\ell_p$  minimization ( $p < 1$ ) by Peng et al. (2024) achieves only local convergence.*

#### 4.1.1. Discussion of Assumptions

Assumption 1 ensures that  $L_\star$  contains more points than all other low-dimensional subspaces by some margin. In the Generalized Haystack model discussed below, it is satisfied with probability 1.

Assumption 2 represents a generic condition on the inlier-outlier dataset,  $\mathcal{X}$ , that can be satisfied in a wide variety of settings. We can illustrate distinct examples where the conditions of Assumption 2 hold using two data models inspired by Maunu et al. (2019); Maunu and Lerman (2019). In particular, the condition in Assumption 2 is almost identical to the conditions of these past works, and so we can easily extend their models to our setting.

**Adversarial Model:** For the first example of adversarial outliers as first discussed in Maunu and Lerman (2019), we must define statistics that measure how well conditioned the inliers are. We define the  $d$ -condition numbers of the inliers to be

$$\kappa_2(\mathcal{X}_{\text{in}}) = \frac{\sigma_1(\mathbf{X}_{\text{in}})^2}{\sigma_d(\mathbf{X}_{\text{in}})^2}, \quad \kappa_1(\mathcal{X}_{\text{in}}) = \frac{\max_{\mathbf{u} \in L_\star \cap S^{D-1}} \sum_{\mathbf{x} \in \mathcal{X}_{\text{in}}} |\mathbf{u}^T \mathbf{x}|}{\min_{\mathbf{u} \in L_\star \cap S^{D-1}} \sum_{\mathbf{x} \in \mathcal{X}_{\text{in}}} |\mathbf{u}^T \mathbf{x}|}$$

where  $\mathbf{X}_{\text{in}} \in \mathbb{R}^{D \times n}$  is a matrix with the inlier points as columns. These quantities measure how well spread the inliers are within the underlying subspace  $L_\star$  with respect to different norms.

**Remark 5.** *Consider the case where inliers follow a Gaussian distribution  $N(\mathbf{0}, \mathbf{P}_{L_\star})$ . Then, with high probability, it is not hard to show that  $\kappa_2(\mathcal{X}_{\text{in}})$  and  $\kappa_1(\mathcal{X}_{\text{in}})$  concentrate around 1 as  $n_{\text{in}} \rightarrow \infty$  (Vershynin, 2010, 2018). When the inliers follow a general Gaussian distribution  $N(\mathbf{0}, \mathbf{\Sigma}_{\text{in}})$ ,  $\kappa_2(\mathcal{X}_{\text{in}})$  concentrates around  $\lambda_1(\mathbf{\Sigma}_{\text{in}})/\lambda_d(\mathbf{\Sigma}_{\text{in}})$  and  $\kappa_1(\mathcal{X}_{\text{in}})$  concentrates around  $\sqrt{\lambda_1(\mathbf{\Sigma}_{\text{in}})/\lambda_d(\mathbf{\Sigma}_{\text{in}})}$ .*

While we assume that the dataset  $\mathcal{X}$  lies on the sphere, this is without loss of generality, since we can always normalize the points in our dataset before running an RSR algorithm.

**Proposition 1** (Adversarial Outliers). *Suppose that  $\mathcal{X} \subset S^{D-1}$ . Then, Assumption 2 holds if there exists a  $\theta_0$  such that*

$$\frac{n_{\text{in}}}{n_{\text{out}}} \geq \max \left( d \sin(\theta_0) \kappa_2(\mathcal{X}_{\text{in}}) \max(1, \epsilon), \frac{1}{\cos(\theta_0)} \sqrt{d} \kappa_1(\mathcal{X}_{\text{in}}) \right).$$

*Proof of Proposition 1.* Consider an inlier-outlier on the sphere,  $\mathcal{X} \subset S^{D-1}$ . Then, it is not hard to show that  $S_{\text{out}} = |\mathcal{X}_{\text{out}}|$ , which is achieved by outliers lying along a 1-dimensional subspace. On the other hand, for the first condition in Assumption 2, we can bound

$$\sigma_d \left( \frac{\sum_{\mathbf{x} \in \mathcal{X}_{\text{in}}} \mathbf{x} \mathbf{x}^T}{\max(\|\mathbf{x}\|, \epsilon)} \right) \geq \frac{|\mathcal{X}_{\text{in}}|}{d \kappa_2(\mathcal{X}_{\text{in}}) \max(1, \epsilon)}. \quad (21)$$

For the second condition, we bound

$$\min_{\mathbf{u} \in L_* \cap S^{D-1}} \sum_{\mathcal{X}_{\text{in}}} |\mathbf{u}^T \mathbf{x}| \geq \frac{|\mathcal{X}_{\text{in}}|}{\sqrt{d} \kappa_1(\mathcal{X}_{\text{in}})} \quad (22)$$

by the pigeonhole principle. Thus, fixing  $\theta_0$  as a constant, we see that both conditions in Assumption 2 are satisfied once  $n_{\text{in}}/n_{\text{out}} = O(d)$ , where the big-O depends on the conditioning  $\kappa_2(\mathcal{X}_{\text{in}})$  and  $\kappa_1(\mathcal{X}_{\text{in}})$ . This matches the result of Maunu and Lerman (2019) with potentially better dependence on the conditioning of  $\mathcal{X}_{\text{in}}$ . On the other hand, if the inliers follow a distribution  $N(\mathbf{0}, \mathbf{P}_L)$ , then  $\kappa_2(\mathcal{X}_{\text{in}})$  and  $\kappa_1(\mathcal{X}_{\text{in}})$  are  $O(1)$  with high probability. Thus choosing  $\theta_0 = \arcsin(1/\sqrt{d})$ , we can actually achieve  $n_{\text{in}}/n_{\text{out}} = O(\sqrt{d})$ .  $\square$

**Generalized Haystack model:** Another common approach to analyzing deterministic conditions is to assume a statistical model and identify regimes where they hold. Prior works often use the Haystack Model (Lerman et al., 2015) or its generalized variant (Maunu et al., 2019).

Here we recall the Generalized Haystack model Maunu et al. (2019): we assume that  $\mathbf{x} \in \mathcal{X}$  are i.i.d. sampled from distribution  $\mu = \alpha_0 \mu_0 + \alpha_1 \mu_1$ , that is, it is sampled from  $\mu_0$  with probability  $\alpha_0$  and sampled from  $\mu_1$  with probability  $\alpha_1$ , where  $\alpha_0 + \alpha_1 = 1$ . In particular,  $\mu_1$  is the distribution of inliers and is assumed to be  $N(0, \Sigma_{\text{in}}/d)$ , and  $\mu_0$  is the distribution of outliers and is assumed to be  $N(0, \Sigma_{\text{out}}/D)$ . In addition, we assume that  $\Sigma_{\text{in}} \succeq \sigma_{\text{in}}^2 \mathbf{P}_{L_*}/d$  and  $\Sigma_{\text{out}} \preceq \sigma_{\text{out}}^2 \mathbf{I}/D$ , and their condition numbers are bounded by  $O(1)$ . With this model, we prove Assumption 2 holds in the following proposition.

**Proposition 2** (Generalized Haystack Model). *Suppose that inliers and outliers follow the Generalized Haystack model. Then, if  $n = O(D^3 \log(D))$ , Assumption 2 holds with high probability once  $\frac{n_{\text{in}}}{n_{\text{out}}} = O\left(\frac{\sigma_{\text{out}}}{\sigma_{\text{in}}} \frac{d}{\sqrt{D(D-d)}}\right)$ .*



For a proof, see Section 6.3. This matches the sharpest bounds for low sample sizes, see Zhang and Lerman (2014); Hardt and Moitra (2013); Maunu et al. (2019). On the other hand, one could also consider an asymptotic regime as in Lerman and Maunu (2018a); Maunu et al. (2019), where it is possible to take the ratio  $n_{\text{in}}/n_{\text{out}}$  to zero for fixed  $d$  and  $D$  as  $n \rightarrow \infty$  in the Haystack model, where  $\Sigma_{\text{in}} = \mathbf{P}_{L_\star}/d$  and  $\Sigma_{\text{out}} = \mathbf{I}/D$ .

#### 4.1.2. Extensions of Theory

There exist a couple of straightforward extensions of our theoretical results that we do not include in this paper.

**Stability to noise:** The FMS-DS algorithm exhibits empirical stability to noise. Our analysis can be extended to show that FMS-DS converges to a neighborhood of  $L_\star$  since any  $L$  outside this neighborhood can not be a fixed point. Technical analysis is deferred to future work.

**Fixed smoothing parameters:** FMS algorithm (Maunu et al., 2019) uses the fixed value  $\epsilon_k = \epsilon$  for  $k \geq 1$ . However, they are only able to guarantee convergence for the Haystack model. A corollary of Theorem 1 allows us to give a more general guarantee of linear convergence of FMS under our generic conditions. Its proof follows from the proof of Lemma 3, and it also implies that all stationary points of the regularized objective function  $F_\epsilon(\mathbf{x})$  lie within a small neighborhood of  $L_\star$ .

**Corollary 1** (Global convergence of FMS with fixed  $\epsilon$ ). *Under the Assumptions 1 and 2 and if  $\epsilon_k = \epsilon$  for all  $k \geq 1$ , then in  $2\left\|\sum_{\mathbf{x} \in \mathcal{X}} \mathbf{x}\mathbf{x}^T\right\| \frac{F_\epsilon(L^{(0)}) - F(L_\star)}{\epsilon S_{\text{in}} \cos \theta_0 - S_{\text{out}}}$  iterations, FMS reaches a subspace  $L^{(k)}$  satisfying  $q_{0.5}(\{\text{dist}(\mathbf{x}, L^{(k)})\}_{\mathbf{x} \in \mathcal{X}_{\text{in}}}) \leq \epsilon$ .*

#### 4.2. Affine Subspace Recovery

This section presents a local theoretical guarantee for the AFMS-DS algorithm in Section 3.2. While weaker than Theorem 1 due to stricter assumptions, it is, to our knowledge, the first theoretical guarantee for robust affine subspace estimation.

We now present our assumptions for the main theorem on affine subspace recovery. First, we assume WLOG that  $\mathbf{m}_\star = 0$  due to the translation equivariance of the IRLS method. Second, the following assumption generalizes Assumption 1 to the affine setting.

**Assumption 3.** *For all  $d - 1$ -dimensional affine subspaces  $[A_0] \subset [A_\star]$  and  $d$ -dimensional affine subspaces  $[A] \neq [A_\star]$  in  $\mathcal{A}(D, d)$ ,  $|\mathcal{X} \cap ([A_0] \cup [A])|/|\mathcal{X}| < \gamma < \gamma_\star/2$ .*

Finally, we also have a generalization of our generic condition in Assumption 2 to the affine setting. To do this, we define a notion of distance between a representative  $A = (L, \mathbf{m}) \in \mathcal{G}(D, d) \times$

$\mathbb{R}^D$  and an equivalence class  $[A'] = [(L', \mathbf{m}')] \in \mathcal{A}(D, d)$ :

$$\text{dist}(A, [A']) = \sqrt{\sum_{i=1}^d \theta_i^2(L, L') + \text{dist}^2(\mathbf{m}, [A'])}, \quad (23)$$

where  $\text{dist}(\mathbf{m}, [A']) = \text{dist}(\mathbf{m} - \mathbf{m}', L')$ . We discuss this more in Section 4.2.1.

**Assumption 4.** *There exists  $c_0 < \pi/2$  such that for any  $[A] \in \mathcal{A}(D, d)$  such that  $\text{dist}(A_\star, [A]) = \text{dist}((L_\star, 0), [A]) \leq c_0$ , then*

$$\frac{1}{\cos^2 c_0} \sum_{\mathbf{x} \in \mathcal{X}'_{\text{in}}} \text{dist}(\mathbf{x}, [A]) \geq \max 4 \left( \frac{\pi}{2} \sum_{\mathbf{x} \in \mathcal{X}_{\text{out}}} \text{dist}(\mathbf{P}_{L_\star} \mathbf{x}, [A]), \theta_1(L, L_\star)^2 \left\| \mathbf{P}_{L_\star}^\perp \sum_{\mathbf{x} \in \mathcal{X}_{\text{out}}} \mathbf{x} \mathbf{x}^T \mathbf{P}_{L_\star}^\perp \right\| \right). \quad (24)$$

In Assumption 4, (49) implies that no subspace  $[A]$  contains too many inliers, and (24) implies that the influence of the inliers is larger than that of the outliers. Compared with the assumptions for Theorem 1, these assumptions are more restrictive.

Our main theoretical result on AFMS-DS guarantees that it converges locally and can be viewed as a generalization of Theorem 1.

**Theorem 2.** *[Local convergence of AFMS-DS] Under Assumptions 3 and 4 and  $\text{dist}(A_\star, [A^{(k)}]) \leq c_0$  for all  $k \geq 1$ , where  $A^{(k)}$  is the sequence generated by AFMS-DS, then  $[A^{(k)}]$  converges to  $[A_\star]$ . In addition, the sequence  $F_{\epsilon_k}(A^{(k)})$  is nonincreasing and converges to  $F(A_\star)$  linearly.*

The proof is a natural extension of the argument presented in Theorem 1 and is provided in Section 6.2. However, in the affine setting, the assumption (24) becomes more challenging to simplify. Consequently, our result relies on a stronger condition, namely that  $\text{dist}(A_\star, [A^{(k)}]) \leq c_0$  for all  $k \geq 1$ .

We note, however, that by following the proof of Theorem 1, if the initialization is chosen such that  $F_{\epsilon_0}(A^{(0)})$  is sufficiently small (see definition of  $F_\epsilon(A)$  in (43)), then this condition can be satisfied. As a result, a “good initialization” assumption is sufficient for the convergence of AFMS-DS.

We conjecture that further analysis may yield results analogous to Assumption 2, potentially leading to global convergence guarantees. We leave this investigation for future work.

#### 4.2.1. Discussion of Assumption 4

Following the discussion in Section 4.1.1, we analyze Assumption 4 under both the adversarial and Haystack models. Unlike the earlier spherical setting, we do not consider sphereized models here, as they are not well-suited for affine subspace recovery.

Instead, we adopt a probabilistic framework in which a fraction  $\alpha_{\text{in}}$  of the samples are inliers and  $\alpha_{\text{out}} = 1 - \alpha_{\text{in}}$  are outliers. Inliers are drawn from the distribution  $\mu_{\text{in}} = \mathcal{N}(0, \Sigma_{\text{in}}/d)$ , where

$\Sigma_{\text{in}}$  is a positive semidefinite matrix with range in  $L_*$  and  $\sigma_d(\Sigma_{\text{in}}) \geq 1$ . Outliers are either drawn from a general distribution  $\mu_{\text{out}}$  (affine adversarial model), or from a Gaussian  $\mathcal{N}(0, \Sigma_{\text{out}}/D)$  with  $\Sigma_{\text{out}} \preceq \sigma_{\text{out}}^2 \mathbf{I}$  (Affine Haystack model).

**Proposition 3** (Affine Adversarial Model). *Under the affine adversarial model, Assumption 4 holds if*

$$\frac{\alpha_{\text{in}}}{\alpha_{\text{out}}} > O \left( \max \left( \sqrt{d} \int_{\mathbf{x} \sim \mu_{\text{out}}} \|P_{L_*} \mathbf{x}\|, 1, c_0 \cos^2(c_0) \sqrt{d} \left\| \int_{\mathbf{x} \sim \mu_{\text{out}}} P_{L_*^\perp} \mathbf{x} \mathbf{x}^\top P_{L_*^\perp} \right\| \right) \right).$$

Proposition 3 suggests that if  $c_0$  is chosen sufficiently small and the distribution  $\mu$  has support of magnitude  $O(1)$ , then the outlier ratio must be bounded by  $O(1/\sqrt{d})$ . This bound is comparable to the term  $\frac{1}{\cos(\theta_0)} \sqrt{d} \kappa_1(\mathcal{X}_{\text{in}})$  in Proposition 1. The second condition in Proposition 1 corresponds to the first inequality in (12), which we do not analyze here, since our analysis assumes  $c_0$  is sufficiently small.

**Proposition 4** (Affine Haystack Model). *Under the adversarial Haystack model, and assuming  $\sigma_{\text{out}} \leq \sqrt{D/d}$ , Assumption 4 and equation (24) hold provided that*

$$\frac{\alpha_{\text{in}}}{\alpha_{\text{out}}} \geq \max \left( 1, O(c_0 \frac{\sqrt{d}}{D} \sigma_{\text{out}}^2) \right).$$

We note that the required inlier fraction for the Affine Haystack model is  $O(1)$ , in contrast to the  $O(d/D)$  requirement in the Generalized Haystack model discussed in Section 4.1.1. However, the Affine Haystack model allows outliers to have magnitudes up to a factor of  $\sqrt{D/d}$  larger.

The  $O(1)$  inlier requirement is intuitive. For instance, in the case of estimating a 0-dimensional affine subspace (i.e., computing the median), the breakdown point is 0.5, meaning that at least half of the data must be inliers for robust recovery. However, since the outliers in the Affine Haystack model are relatively benign, we expect the breakdown point of AFMS to be lower. We leave a precise characterization of this threshold to future work.

**Discussion of Distance:** For our analysis, we assume that the set of inliers  $\mathcal{X}_{\text{in}}$  lies on a  $d$ -dimensional affine subspace  $[A_*] = [(L_*, \mathbf{m}_*)]$ . This defines a distance between a representative for  $[A]$  and the affine subspace  $[A']$ . To our knowledge, this notion of distance is new in the literature and may be of independent interest. This is not a true metric on the affine Grassmannian since it depends on the choice of  $\mathbf{m}$  in the representation for  $[A]$ . Note, however, that  $\text{dist}(A, [A']) = 0$  if and only if  $[A] = [A']$ .

## 5. Numerical Simulations

In this section, we present experiments on synthetic and real data. Our first experiment in Section 5.1 compares the FMS algorithm with various competitive RSR methods. The second and third

experiments in Sections 5.2 and 5.3 investigate the performance of FMS under various regularization strategies, highlighting the effectiveness of the proposed dynamic smoothing approach in escaping saddle points. The final experiment demonstrates the practical utility of FMS dimensionality reduction in training neural networks. The code used for our experiments and implementations is available at: <https://github.com/alp-del/Robust-PCA>.

### 5.1. Experiment 1: Subspace Recovery Across Methods

For the first experiment, we evaluate the performance of four competitive RSR algorithms on synthetic datasets generated under a semi-adversarial inlier-outlier model. The algorithms chosen are RANSAC (Maunu and Lerman, 2019), STE (Yu et al., 2024), TME (Zhang, 2016), and FMS. We also include PCA as a baseline subspace recovery method. Comparisons with other RSR algorithms have been conducted in prior work and consistently show inferior performance across a range of regimes (see, e.g., Lerman and Maunu (2018b)), especially when one is interested in exact recovery. Although RANSAC and TME were not originally developed for RSR, we use their RSR-adapted versions in our experiments. Finally, we note that the most common implementation of DPCP (Zhu et al., 2018) is equivalent to FMS, but targets the orthogonal complement of the desired subspace. As a result, it yields the same solution as FMS when using the same initialization and parameters.

The inlier-outlier models used here aim to demonstrate the performance of these RSR algorithms in a semi-adversarial setting. The datasets consist of two components: inliers lying on a subspace of dimension  $d \in \{3, 10\}$  and sampled from a standard Gaussian distribution supported on that subspace, and outliers lying on a separate subspace of dimension  $d_{\text{out}} \in \{1, 5, 10\}$  and independently sampled from a standard Gaussian distribution supported on the outlier subspace. WLOG, we assume that the ambient dimension is  $D = d + d_{\text{out}}$ . As a final step, we normalize all points so that they lie on the unit sphere in  $\mathbb{R}^D$  to remove effects of scale.

The goal is to compare the performance of the RSR algorithms in these semi-adversarial settings. Therefore, we fix the total number of data points at  $n = 160$ , and we vary the proportion of inliers and outliers to see where each algorithm breaks down.

Since we are comparing iterative algorithms, we ensure a fair comparison of running times by setting the maximum number of iterations to 200 for the RANSAC, FMS, TME, and STE methods. In particular, we emphasize that RANSAC is executed with only 200 candidate samples. This choice is motivated by the fact that the computational complexity of a single iteration of FMS or STE is comparable to that of evaluating one candidate sample in RANSAC.

For the STE method, we use a gamma parameter of 2, and for TME we use regularization of  $\epsilon = 10^{-10}$ . We run FMS with fixed  $\epsilon = 10^{-10}$ , as well as dynamic smoothing with two choices

of  $\gamma = 0.5$  and  $\gamma = 0.1$ . To ensure statistical reliability, we generate 200 datasets for each pair  $d$  and  $d_{\text{out}}$ , and the average performance is reported. FMS and STE are initialized using the PCA subspace, and TME is initialized with the sample covariance.

Let the orthonormal matrix  $\mathbf{P} \in \mathbb{R}^{D \times d}$  represent the basis of the true inlier subspace, and let  $\tilde{\mathbf{P}} \in \mathbb{R}^{D \times d}$  denote the basis of the estimated subspace. We measure the subspace estimation error by  $\|\tilde{\mathbf{P}}\tilde{\mathbf{P}}^\top - \mathbf{P}\mathbf{P}^\top\|_2$ , which corresponds to the sine of the largest principal angle between the true subspace and its estimate. Due to the fact that we are in a noiseless regime, we plot all errors on a log scale. Since error is reported as the geometric mean of the errors over the 200 datasets, the result is the averaged log-error.

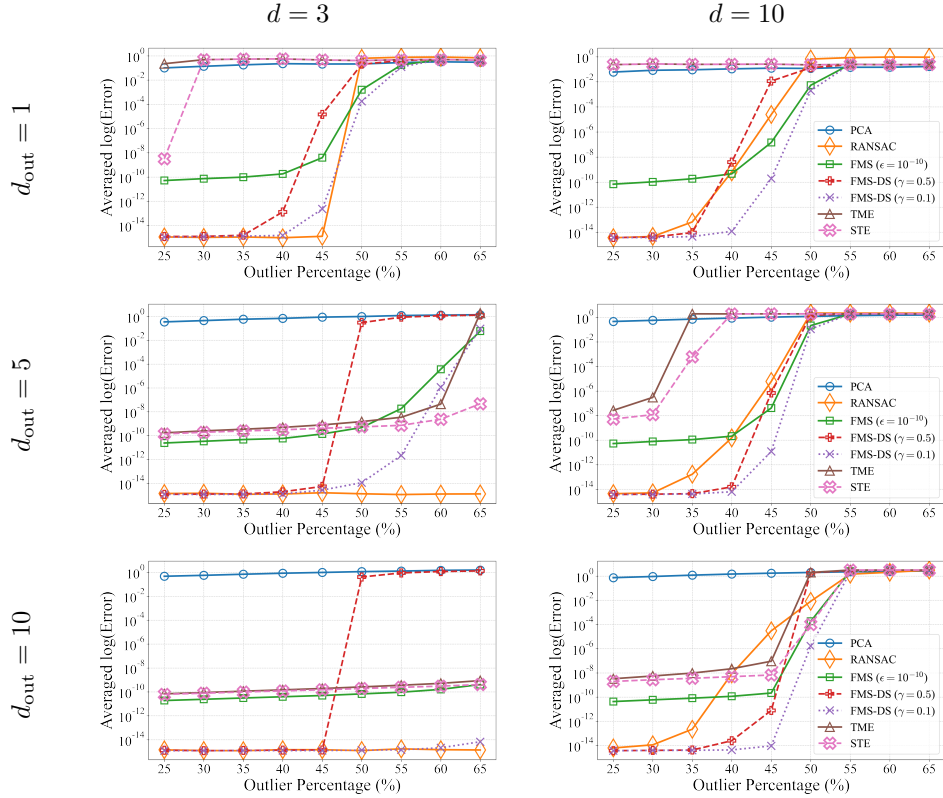


Figure 1: Performance comparison of PCA, TME, RANSAC, STE, and FMS on synthetic data, reporting the geometric mean of the error over 200 repetitions on a log scale. This corresponds to the averaged log-error. We vary outlier dimension across rows and inlier dimension across columns as follows: top row: outlier dimension  $d_{\text{out}} = 1$ , middle row:  $d_{\text{out}} = 5$ , bottom row:  $d_{\text{out}} = 10$ . Left column: inlier dimension  $d = 3$ , right column:  $d = 10$ . As we can see, FMS-DS with small  $\gamma$  performs well across a range of settings. RANSAC performs well for small  $d$ , but fails for larger  $d$  due to the fact that its runtime is exponential in  $d$ , and we cap the number of iterations.

As illustrated in Figure 1, FMS has a comparable performance as STE and TME and usually outperforms them, particularly when the inlier dimension is higher. RANSAC, which follows a

fundamentally different approach, performs well in low-dimensional settings but degrades significantly as dimensionality increases. This is because RANSAC estimates candidate subspaces from randomly selected sets of  $d$  samples, and its success depends on all  $d$  samples being inliers. This condition becomes exponentially unlikely as  $d$  grows larger.

Since STE, FMS, and TME are applied with fixed regularization parameters, as no dynamic smoothing schemes are available for them, they do not reach machine precision. On the other hand, applying FMS with fixed  $\epsilon = 10^{-15}$  has the same performance as FMS-DS with  $\gamma = 0.1$ .

### 5.2. Experiment 2: Effect of Regularization in FMS

We investigate how different regularization strategies influence the performance of FMS in a setting where the initialization is chosen adversarially. In particular, we aim to demonstrate that dynamic smoothing can avoid saddle points that FMS with fixed regularization may become stuck at.

We compare the following variants:

- FMS with fixed regularization parameters of  $\epsilon = 10^{-3}$ ,  $10^{-10}$ , and  $10^{-15}$ .
- FMS-DS where  $\epsilon$  is chosen by (4) with  $\gamma = 0.1$  and  $0.5$ . Here, we set the initial value  $\epsilon^{(0)}$  to be the  $\gamma$ -quantile of the  $\{\text{dist}(\mathbf{x}, L_0)\}_{\mathbf{x} \in \mathcal{X}}$ , where  $L_0$  represents the initial subspace.

Similar to Experiment 1, the synthetic dataset is constructed with an inlier subspace dimension of  $d = 3$  and an outlier dimension of  $d_{\text{out}} = 1$ . The ambient space has dimension  $D = d + d_{\text{out}} = 4$ . The dataset contains a total of 200 data points. To demonstrate that the dynamic smoothing strategy can escape local minima or stationary points, we initialize the algorithm at a stationary point of the FMS objective—specifically, a subspace orthogonal to the true underlying subspace and contains the outliers. We again generate 200 datasets in this model and average the results for each algorithm.

Figures 2 and 3 report the results of this experiment. In Figure 2, we report the averaged log-error of the different methods as a function of outlier percentage. We also report failure rate, which corresponds to FMS getting stuck at a bad stationary point, as a function of outlier percentage in Figure 3. As shown in these figures, FMS-DS with larger  $\gamma$  significantly outperforms both fixed regularization approaches, regardless of the fixed regularization strength.

It is worth noting that FMS with a large regularization parameter consistently results in higher error due to the overly strong regularization. On the other hand, while FMS with small regularization can perform well in some cases, it begins to fail when the inlier percentage is  $\geq 12\%$ , in part because it becomes trapped in stationary points. In contrast, FMS with dynamic smoothing achieves consistently better performance across a range of outlier ratios.

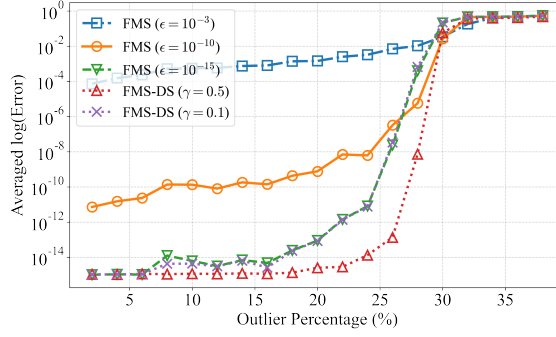


Figure 2: Averaged log-error versus outlier percentage for the experiment with adversarial initialization. Here, the inlier subspace dimension is 3 and the outlier subspace is a 1-dimensional subspace orthogonal to it. FMS is initialized with 2 directions within the inlier subspace and one direction orthogonal to it. Left: boxplot of the errors. Right: geometric mean of the errors.

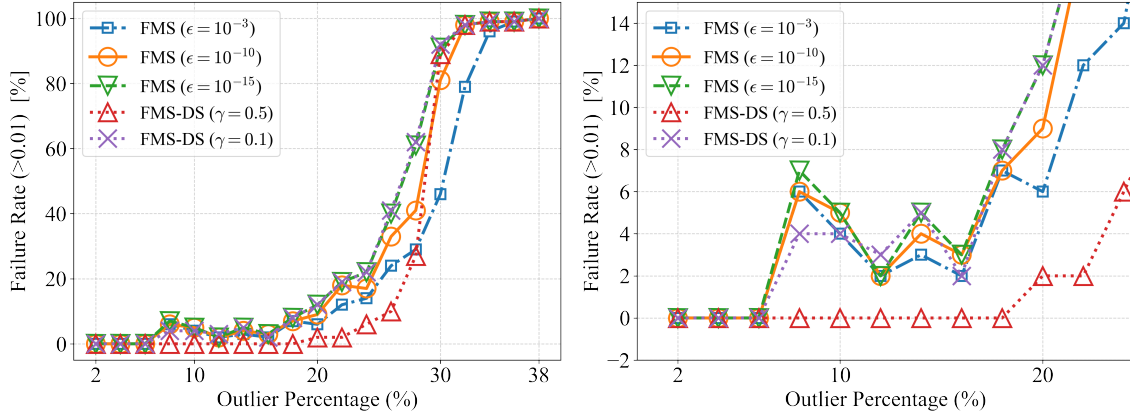


Figure 3: Failure rate of the various FMS algorithms under the same setting as Figure 2. Left: failure rate versus outlier percentage. Right: zoomed in view.

### 5.3. Experiment 3: Iteration-Wise Error Analysis

We further investigate the convergence behavior of FMS by plotting the estimation error over iterations for each regularization strategy. We follow the settings of  $d$  and  $d_{\text{out}}$  from Experiment 2, but fix the number of inliers at 100 and outliers at 30. The algorithm is initialized using the PCA subspace as in Experiment 1, or the orthogonal subspace as in Experiment 2.

The left display of Figure 4 shows that dynamic regularization achieves the lowest estimation error, continuously decreasing until it reaches machine precision. The rate of convergence is slightly slower than FMS with small regularization ( $\epsilon = 10^{-15}$ ). In contrast, for FMS with larger fixed regularization, the estimation error plateaus once it reaches the same order of magnitude as the regularization parameter, indicating that fixed regularization introduces bias into the estimation. The right display of Figure 4 demonstrates the performance of the various regularization strategies

with the poor initialization of Experiment 2. As we can see, FMS-DS with  $\gamma = 0.5$  and FMS with fixed  $\epsilon = 10^{-3}$  are more effective at escaping the saddle point. However, the fixed regularization is not able to adapt and plateaus at the fixed error of  $\approx 10^{-3}$  while FMS-DS converges to the global solution. FMS-DS with small gamma and FMS with small fixed  $\epsilon$  perform comparably.

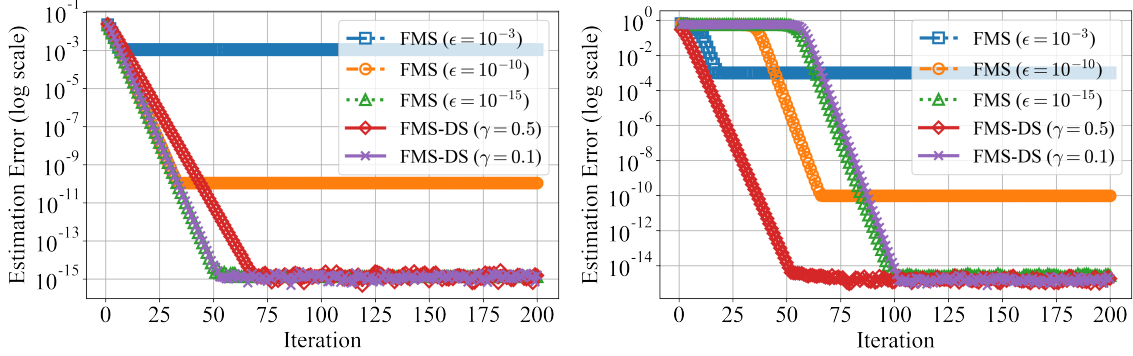


Figure 4: Averaged log-error versus iteration for FMS with different regularization strategies. On the left, we demonstrate convergence with PCA initialization, and on the right, we demonstrate convergence with the orthogonal initialization of Experiment 2. The left plot demonstrates that in settings with good initialization and lack of bad stationary points, FMS with small fixed  $\epsilon$  and FMS-DS with small  $\gamma$  both perform well. On the other hand, for bad initialization, we see that FMS with large  $\epsilon$  and FMS-DS with large  $\gamma$  are better at escaping the saddle point. Out of these two, only FMS-DS can exactly recover the underlying subspace.

#### 5.4. A Practical Demonstration of the FMS Algorithm

While the previous section provides a new theoretical analysis of the FMS algorithm and extends it to affine settings, this analysis applies only in inlier-outlier settings. However, it is typically unknown a priori whether a dataset satisfies this condition. To further motivate the FMS algorithm and its role in robust subspace estimation, we present an application related to low-dimensional neural network training.

A line of work studies the use of a subspace-constrained optimization. One example is neural network training, where Li et al. (2022) use Dynamic Linear Dimensionality Reduction (DLDR) to show that training in a PCA subspace can improve generalization. Unfortunately, this procedure of subspace estimation lies at odds with the current understanding of neural network training. We argue that using vanilla PCA may be misguided since recent evidence indicates that stochastic gradient descent in neural network training exhibits heavy-tailed noise Simsekli et al. (2019); Zhou et al. (2020).

The implementation details of DLDR are as follows (Li et al., 2022). First, during training with SGD, we sample  $t$  steps of neural network parameters  $\{\mathbf{w}_1, \mathbf{w}_2, \dots, \mathbf{w}_t\} \subset \mathbb{R}^D$ . The weights are



then centered by subtracting the mean, and the PCA subspace is computed. The network is then retrained, with gradients projected to the PCA subspace.

Motivated by this, we replace the PCA subspace in the previous procedure with FMS and AFMS. For completeness, we also report the application of TME, PCA, and spherical PCA (SPCA), which computes the PCA subspace of the normalized dataset  $\mathbf{x}/|\mathbf{x}| : \mathbf{x} \in \mathcal{X}$  (Locantore et al., 1999). We do not report dynamic smoothing, as it did not change the performance of FMS. In particular, dynamic smoothing typically affects the algorithm’s rate of convergence and precision, but neither is essential in this example.

Specifically, we trained CIFAR-10 (Krizhevsky, 2009) on ResNet-20, CIFAR-100 (Krizhevsky, 2009) on ResNet-32, and Tiny-ImageNet (Deng et al., 2009) on ResNet-18. The **CIFAR-10** dataset consists of 60,000 color images of size  $32 \times 32$  pixels, categorized into 10 classes. It contains 50,000 training images and 10,000 test images. The **CIFAR-100** dataset is an extension of CIFAR-10, containing 100 classes instead of 10. Each class has 600 images, making a total of 60,000 images. The dataset consists of 50,000 training images and 10,000 test images of size  $32 \times 32$  pixels. The **Tiny ImageNet** dataset contains 200 classes with images resized to  $64 \times 64$  pixels. It includes 100,000 training images and 10,000 validation images.

For all three data sets, the images were normalized using their channel-wise means and variances. The deep neural networks were trained with the SGD optimizer using a weight decay of  $1e-4$ , a momentum of 0.9, and a batch size of 128. The learning rate was initially set to 0.1 and decayed to 0.01 over 100 epochs. Model parameters were sampled at the end of every epoch, after which FMS, PCA, and TME were applied to estimate the subspace. When training within this subspace using projected-SGD, we maintained the same batch size and momentum as in the original SGD setup. The learning rate was set to 1 initially and decayed to 0.1 over 30 epochs.

To assess robustness, we introduced additional label corruption by randomly selecting a fraction of the training data and assigning random labels to them. The testing accuracies of our simulations are visualized in Figure 5. The first row illustrates the accuracies of all methods applied to three datasets reduced to 20 dimensions, while the second row shows the accuracies when a corruption level of 0.15 is applied. Note that AFMS and FMS have the same performance in all scenarios. PCA and TME also perform similarly. As shown in Figure 5, label corruption significantly degrades the performance of SGD. In contrast, training in low-dimensional subspaces demonstrates that FMS outperforms the other methods.

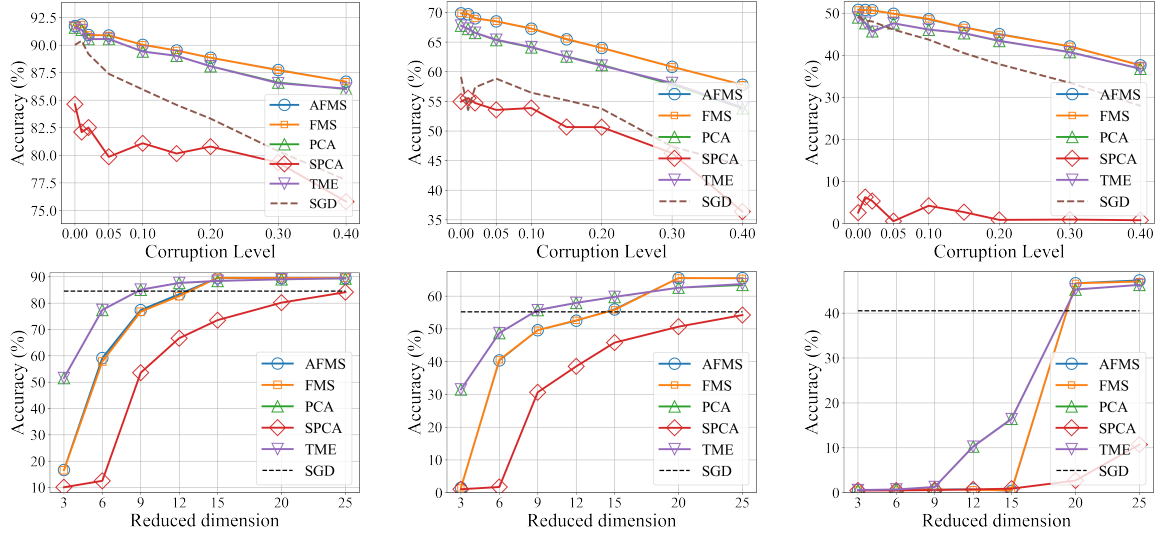


Figure 5: Comparison of PCA, SPCA, TME, FMS, and AFMS for low-dimensional neural network training using three different datasets (left: CIFAR-10, center: CIFAR-100, right: Tiny ImageNet). Top row: subspace dimension fixed at 20 and varying corruption, bottom row: corruption level fixed at 0.15 and varying subspace dimension. As we can see, for sufficiently large dimensions, the (A)FMS subspace outperforms the subspace found by other subspace recovery methods.

## 6. Additional Proofs

In this section, we provide additional proofs that were deferred for readability. Section 6.1 contains the proofs of Lemmas 1–5, which were stated during the proof of Theorem 1. Section 6.2 presents the proof of Theorem 2, which builds upon the ideas used in the proof of Theorem 1. Lastly, Section 6.3 provides the proof of Proposition 2, and Section 6.4 provides the proofs of Propositions 3 and 4.

### 6.1. Proof of Supplementary Lemmas for Theorem 1

*Proof of Lemma 1.* Assume that  $\epsilon_1 < \epsilon_2$ . We remind ourselves that

$$F_\epsilon(L) = \sum_{\mathbf{x} \in \mathcal{X}: \text{dist}(\mathbf{x}, L) > \epsilon} \text{dist}(\mathbf{x}, L) + \sum_{\mathbf{x} \in \mathcal{X}: \text{dist}(\mathbf{x}, L) \leq \epsilon} \left( \frac{1}{2}\epsilon + \frac{\text{dist}(\mathbf{x}, L)^2}{2\epsilon} \right).$$

We proceed by cases for each  $\mathbf{x}$ .

If  $\text{dist}(\mathbf{x}, L) > \epsilon_2$ , then the corresponding term in  $F_{\epsilon_1}$  is equal to the term in  $F_{\epsilon_2}$ . Similarly, if  $\text{dist}(\mathbf{x}, L) \leq \epsilon_1$ , then the term is again equal. It remains to study the case where  $\epsilon_1 < \text{dist}(\mathbf{x}, L) \leq \epsilon_2$ . The result follows from the fact that

$$|z| \leq \frac{\epsilon}{2} + \frac{z^2}{2\epsilon}$$

for all  $\epsilon > 0$ . In particular, WLOG assume  $z > 0$ , and the inequality is equivalent to

$$z^2 + \epsilon^2 - 2z\epsilon = (z - \epsilon)^2 \geq 0.$$

□

*Proof of Lemma 2.* Before proving Lemma 2, we prove the following lemma on the quadratic growth of the trace function.

**Lemma 6.** *For a function  $f : \mathcal{G}(D, d) \rightarrow \mathbb{R}$  defined by  $f(L) = \text{tr}(\mathbf{P}_L \mathbf{\Sigma})$ . Let  $L_\star = \arg \max_L f(L)$ , then*

$$f(L_\star) - f(L) \geq \frac{\|\mathbf{P}_L \mathbf{\Sigma} \mathbf{P}_{L^\perp}\|_F^2}{\|\mathbf{\Sigma}\|}.$$

*Proof of Lemma 6.* In the proof we denote

$$\mathbf{S}_{L_1, L_2} = \mathbf{U}_{L_1}^\top \mathbf{\Sigma} \mathbf{U}_{L_2}.$$

We note that

$$\mathbf{\Sigma} - \mathbf{S}_0 := \begin{pmatrix} [\mathbf{\Sigma}]_{L, L} & [\mathbf{\Sigma}]_{L, L^\perp} \\ [\mathbf{\Sigma}]_{L^\perp, L} & [\mathbf{\Sigma}]_{L^\perp, L^\perp} ([\mathbf{\Sigma}]_{L, L})^{-1} [\mathbf{\Sigma}]_{L, L^\perp} \end{pmatrix}$$

is nonnegative definite, and in addition,  $f(L_\star)$  is the sum of the first  $d$  singular values of  $\mathbf{\Sigma}$ . As a result

$$f(L_\star) = \sum_{i=1}^d \sigma_i(\mathbf{\Sigma}) \geq \sum_{i=1}^d \sigma_i(\mathbf{S}_0) = \text{tr}(\mathbf{S}_0) = \text{tr}([\mathbf{\Sigma}]_{L, L}) + \text{tr}([\mathbf{\Sigma}]_{L^\perp, L^\perp} ([\mathbf{\Sigma}]_{L, L})^{-1} [\mathbf{\Sigma}]_{L, L^\perp}), \quad (25)$$

where the second equality follows from the fact that  $\text{rank}(\mathbf{S}_0) = d$ .

In addition,

$$\begin{aligned} \text{tr}([\mathbf{\Sigma}]_{L^\perp, L^\perp} ([\mathbf{\Sigma}]_{L, L})^{-1} [\mathbf{\Sigma}]_{L, L^\perp}) &= \|[\mathbf{\Sigma}]_{L^\perp, L} ([\mathbf{\Sigma}]_{L, L})^{-1/2}\|_F^2 \\ &\geq \|[\mathbf{\Sigma}]_{L^\perp, L}\|_F^2 / \|[\mathbf{\Sigma}]_{L, L}\| \\ &\geq \|[\mathbf{\Sigma}]_{L^\perp, L}\|_F^2 / \|\mathbf{\Sigma}\|. \end{aligned}$$

Recalling that  $f(L) = \text{tr}([\mathbf{\Sigma}]_{L, L})$ , the lemma is proved. □

We now proceed with the proof of Lemma 2.

To prove Lemma 2, we use an auxiliary function defined as follows:

$$\begin{aligned} G_\epsilon(L, L_0) &= \sum_{\mathbf{x} \in \mathcal{X} : \text{dist}(\mathbf{x}, L_0) > \epsilon} \left( \frac{1}{2} \text{dist}(\mathbf{x}_i, L_0) + \frac{\text{dist}(\mathbf{x}_i, L)^2}{2 \text{dist}(\mathbf{x}_i, L_0)} \right) \\ &\quad + \sum_{\mathbf{x} \in \mathcal{X} : \text{dist}(\mathbf{x}, L_0) \leq \epsilon} \left( \frac{1}{2} \epsilon + \frac{\text{dist}(\mathbf{x}_i, L)^2}{2\epsilon} \right). \end{aligned} \quad (26)$$

Our proof is then based on Lemma 1, Lemma 6, and the following observations (see Lerman and Maunu (2018a) for proof):

$$F_\epsilon(L) = G_\epsilon(L, L) \quad (27)$$

$$F_\epsilon(L_0) \leq G_\epsilon(L, L_0) \text{ with equality holds only when } L = L_0$$

$$L^{(k+1)} = \arg \min_L G_{\epsilon_k}(L, L^{(k)})$$

From the observations in (27) we have

$$F_{\epsilon_{k+1}}(L^{(k+1)}) \leq F_{\epsilon_k}(L^{(k+1)}) \leq G_{\epsilon_k}(L^{(k+1)}, L^{(k)}) \leq G_{\epsilon_k}(L^{(k)}, L^{(k)}) = F_{\epsilon_k}(L^{(k)}).$$

This implies that

$$F_{\epsilon_k}(L^{(k)}) - F_{\epsilon_{k+1}}(L^{(k+1)}) \geq G_{\epsilon_k}(L^{(k)}, L^{(k)}) - G_{\epsilon_k}(L^{(k+1)}, L^{(k)}). \quad (28)$$

Now, using the fact that

$$\text{dist}^2(\mathbf{x}_i, L)^2 = \text{tr}(\mathbf{P}_{L^\perp} \mathbf{x}_i \mathbf{x}_i^T \mathbf{P}_{L^\perp}),$$

we can rewrite

$$\begin{aligned} G_{\epsilon_k}(L, L_0) &= \sum_{\mathbf{x} \in \mathcal{X}: \text{dist}(\mathbf{x}, L_0) > \epsilon_k} \left( \frac{1}{2} \text{dist}(\mathbf{x}_i, L_0)^2 + \frac{\text{dist}(\mathbf{x}_i, L)^2}{2 \text{dist}(\mathbf{x}_i, L_0)} \right) + \\ &\quad \sum_{\mathbf{x} \in \mathcal{X}: \text{dist}(\mathbf{x}, L_0) \leq \epsilon_k} \left( \frac{1}{2} \epsilon_k + \frac{\text{dist}(\mathbf{x}_i, L)^2}{2\epsilon} \right) \\ &= \text{tr} \left( \sum_i \frac{\mathbf{P}_{L^\perp} \mathbf{x}_i \mathbf{x}_i^T \mathbf{P}_{L^\perp}}{2 \max(\text{dist}(\mathbf{x}_i, L_0), \epsilon)} \right) + C(L_0) \\ &= \frac{1}{2} \text{tr}(\mathbf{P}_{L^\perp} \mathbf{S}_{L_0, \epsilon_k} \mathbf{P}_{L^\perp}) + C(L_0) \\ &= \frac{1}{2} \left[ \text{tr}(\mathbf{S}_{L_0, \epsilon_k}) - \text{tr}(\mathbf{P}_L \mathbf{S}_{L_0, \epsilon_k} \mathbf{P}_L) \right] + C(L_0) \end{aligned}$$

for some term that only depends on  $L_0$ . Notice that the third line implies that

$$G_{\epsilon_k}(L, L_0) = \frac{1}{2} \text{tr}(\mathbf{S}_{L_0, \epsilon_k} \mathbf{P}_{L^\perp}) + C(L_0),$$

and so we can apply Lemma 6 to find

$$G(L^{(k)}, L^{(k)}) - G_{\epsilon_k}(L^{(k+1)}, L^{(k)}) \geq \frac{1}{2} \frac{\|\mathbf{P}_{L^{(k)}} \mathbf{S}_{L^{(k)}, \epsilon_k} \mathbf{P}_{L^{(k)}^\perp}\|_F^2}{\|\mathbf{S}_{L^{(k)}, \epsilon_k}\|}.$$

Lemma 2 follows by the previous display and (27).  $\square$

*Proof of Lemma 3.* In this proof, we let  $\mathbf{S}_{L, \epsilon} = \mathbf{S}_{L, \epsilon, in} + \mathbf{S}_{L, \epsilon, out}$ , where

$$\mathbf{S}_{L, \epsilon, in} = \sum_{\mathbf{x} \in \mathcal{X}_{in}} \frac{\mathbf{x} \mathbf{x}^T}{\max(\text{dist}(\mathbf{x}, L), \epsilon)}, \quad \mathbf{S}_{L, \epsilon, out} = \sum_{\mathbf{x} \in \mathcal{X}_{out}} \frac{\mathbf{x} \mathbf{x}^T}{\max(\text{dist}(\mathbf{x}, L), \epsilon)},$$

and we will investigate  $\mathbf{P}_L \mathbf{S}_{L,\epsilon,in} \mathbf{P}_{L^\perp}$  and  $\mathbf{P}_L \mathbf{S}_{L,\epsilon,out} \mathbf{P}_{L^\perp}$  separately.

Let respective principal vectors between  $L$  and  $L_\star$  are  $\{\mathbf{u}_j\}_{j=1}^d$  and  $\{\mathbf{v}_j\}_{j=1}^d$  respectively, and  $\{\mathbf{w}_j\}_{j=1}^d$  are unit vectors lie in  $L^\perp$  such that  $\mathbf{v}_j = \cos \theta_j \mathbf{u}_j + \sin \theta_j \mathbf{w}_j$ . Then we will show that there exists  $1 \leq j \leq d$  such that

$$\mathbf{u}_j^T \mathbf{S}_{L,\epsilon,in} \mathbf{w}_j > \frac{\cos \theta_1}{2\sqrt{d}} S_{in}, \quad |\mathbf{u}_j^T \mathbf{S}_{L,\epsilon,out} \mathbf{w}_j| < S_{out}.$$

We begin by analyzing  $\mathbf{S}_{L,\epsilon,out}$ . By definition of  $S_{out}$ , we have

$$\|\mathbf{S}_{L,\epsilon,out}\| < S_{out}$$

and as a result, for all  $1 \leq j \leq d$ ,

$$|\mathbf{u}_j \mathbf{S}_{L,\epsilon,out} \mathbf{w}_j| < S_{out}.$$

We now analyze  $\mathbf{S}_{L,\epsilon,in}$ . Let us investigate  $\mathbf{u}_j^T \mathbf{x} \mathbf{x}^T$  for any  $\mathbf{x} \in \mathcal{X}_{in}$ ,

$$\mathbf{u}_j^T \mathbf{x} = \cos \theta_j \mathbf{v}_j^T \mathbf{x}, \quad \mathbf{w}_j^T \mathbf{x} = \sin \theta_j \mathbf{v}_j^T \mathbf{x} \quad (29)$$

and  $\mathbf{P}_{L^\perp} \mathbf{x} = \sum_{j=1}^d \mathbf{w}_j \mathbf{w}_j^T \mathbf{x}$ , so

$$\text{dist}(\mathbf{x}, L) = \|\mathbf{P}_{L^\perp} \mathbf{x}\| = \sqrt{\sum_{j=1}^d (\mathbf{w}_j^T \mathbf{x})^2} = \sqrt{\sum_{j=1}^d \sin^2 \theta_j (\mathbf{v}_j^T \mathbf{x})^2}. \quad (30)$$

Next, let us analyze

$$\sum_{j=1}^d \tan \theta_j (\mathbf{u}_j \mathbf{S}_{L,\epsilon,in} \mathbf{w}_j).$$

Applying (29) and (30), for an inlier  $\mathbf{x}$ , we have that

$$\sum_{j=1}^d \tan \theta_j \frac{\sin \theta_j \cos \theta_j (\mathbf{v}_j^T \mathbf{x})^2}{\max(\text{dist}(\mathbf{x}, L), \epsilon)} = \frac{\sum_{j=1}^d \sin^2 \theta_j (\mathbf{v}_j^T \mathbf{x})^2}{\max(\text{dist}(\mathbf{x}, L), \epsilon)} = \frac{\text{dist}^2(\mathbf{x}, L)}{\max(\text{dist}(\mathbf{x}, L), \epsilon)}.$$

Recall that  $\epsilon$  is chosen such that for at least half of the inliers,  $\text{dist}(\mathbf{x}, L) \geq \epsilon$ , so

$$\begin{aligned} \sum_{j=1}^d \tan \theta_j (\mathbf{u}_j \mathbf{S}_{L,\epsilon,in} \mathbf{w}_j) &= \sum_{\mathbf{x} \in \mathcal{X}_{in}} \frac{\text{dist}^2(\mathbf{x}, L)}{\max(\text{dist}(\mathbf{x}, L), \epsilon)} \\ &\geq \sum_{\mathbf{x} \in \mathcal{X}_{in}: \text{dist}(\mathbf{x}, L) > \epsilon} \text{dist}(\mathbf{x}, L) \\ &\geq \frac{1}{2} \sum_{\mathbf{x} \in \mathcal{X}_{in}} \text{dist}(\mathbf{x}, L) \\ &\geq \frac{1}{2} S_{in} \sqrt{\sum_{j=1}^d \sin^2 \theta_j}. \end{aligned} \quad (31)$$

Let  $q_j = \sin^2 \theta_j$ , then  $\sqrt{\sum_{j=1}^d q_j c_j}$  is a concave function of the variables  $q_j$ , and

$$\begin{aligned}
\sum_{\mathbf{x} \in \mathcal{X}_{\text{in}}} \text{dist}(\mathbf{x}, L) &= \sum_{\mathbf{x} \in \mathcal{X}_{\text{in}}} \sqrt{\sum_{j=1}^d q_j (\mathbf{v}_j^T \mathbf{x})^2} \\
&\geq \sqrt{\sum_{j=1}^d q_j} \sum_{\mathbf{x} \in \mathcal{X}_{\text{in}}} |\mathbf{v}_j^T \mathbf{x}| \\
&\geq S_{\text{in}} \sqrt{\sum_{j=1}^d q_j} \\
&= S_{\text{in}} \sqrt{\sum_{j=1}^d \sin^2 \theta_j}.
\end{aligned}$$

On the other hand,

$$\frac{\sqrt{\sum_{j=1}^d \sin^2 \theta_j}}{\sum_{j=1}^d \tan \theta_j} \geq \frac{\frac{1}{\sqrt{d}} \sum_{j=1}^d \sin \theta_j}{\frac{1}{\cos \theta_1} \sum_{j=1}^d \sin \theta_j} = \frac{\cos \theta_1}{\sqrt{d}}. \quad (32)$$

As a result, (31) implies that

$$\max_{j=1, \dots, d} \mathbf{u}_j \mathbf{S}_{L, \epsilon, \text{in}} \mathbf{w}_j \geq \frac{S_{\text{in}} \sqrt{\sum_{j=1}^d \sin^2 \theta_j}}{\sum_{j=1}^d \tan \theta_j} \geq \frac{\cos \theta_1}{2\sqrt{d}} S_{\text{in}}.$$

Denoting the index that achieve the maximum above by  $j_0$ , then Lemma 3 is proved by noting that

$$\|\mathbf{P}_L \mathbf{S}_{L, \epsilon} \mathbf{P}_{L^\perp}\|_F \geq \mathbf{u}_{j_0}^T \mathbf{S}_{L, \epsilon} \mathbf{w}_{j_0} \geq \mathbf{u}_{j_0}^T \mathbf{S}_{L, \epsilon, \text{in}} \mathbf{w}_{j_0} - \|\mathbf{S}_{L, \epsilon, \text{out}}\| \geq \frac{\cos \theta_1}{2\sqrt{d}} S_{\text{in}} - S_{\text{out}}.$$

□

*Proof of Lemma 4.* For simplicity denote the principal angles between  $L$  and  $L_\star$  by  $\{\theta_j\}_{j=1}^d$ . Then, we first claim that

$$F_{\text{in}}(L) \geq \frac{\sum_{j=1}^d \sin \theta_j}{\sqrt{d}} S_{\text{in}} \quad (33)$$

$$|F_{\text{out}}(L) - F_{\text{out}}(L_\star)| \leq S_{\text{out}} \sum_{j=1}^d \theta_j. \quad (34)$$

To prove (33), WLOG assuming that the principal vectors of  $L$  and  $L_\star$  be  $\mathbf{u}_1, \dots, \mathbf{u}_d$  and  $\mathbf{v}_1, \dots, \mathbf{v}_d$ . Then all  $\mathbf{x} \in \mathcal{X}_{\text{in}}$  can be written

$$\mathbf{x} = \sum_{j=1}^d x_j \mathbf{v}_j, \text{ where } x_j = \mathbf{v}_j^T \mathbf{x},$$

and the projection to  $L$  can be written as

$$P_L(\mathbf{x}) = \sum_{j=1}^d x_j P_L(\mathbf{v}_j)$$

Note that  $\mathbf{v}_j$  has an angle of  $\theta_j$  with  $L$  and  $\|\mathbf{v}_j - P_L(\mathbf{v}_j)\| = \sin \theta_j$ , we have

$$\text{dist}(\mathbf{x}, L) = \|\mathbf{x} - P_L \mathbf{x}\| = \sqrt{\sum_{j=1}^d \sin^2 \theta_j x_j^2} = \sqrt{\sum_{j=1}^d \sin^2 \theta_j (\mathbf{v}_j^T \mathbf{x})^2} \geq \frac{1}{\sqrt{d}} \sum_{j=1}^d \sin \theta_j |\mathbf{v}_j^T \mathbf{x}|$$

Summing the above inequality over all  $\mathbf{x} \in \mathcal{X}_{\text{in}}$  and applying the definition of  $S_{\text{in}}$ , (33) is proved.

To prove (34), let  $\{\mathbf{u}_1, \dots, \mathbf{u}_d, \mathbf{w}_1\} \in \mathbb{R}^D$  be an orthonormal set, and let  $L(t) = \text{Sp}(\cos t\theta \mathbf{u}_1 + \sin t\theta \mathbf{w}_1, \mathbf{u}_2, \dots, \mathbf{w}_d)$ . We first notice that

$$\begin{aligned} \left| \frac{d}{dt} \text{dist}(\mathbf{x}, L(t)) \right|_{t=0} &= 2\theta \left| \frac{(\cos t\theta \mathbf{u}_1 + \sin t\theta \mathbf{w}_1)^T \mathbf{x} \mathbf{x}^T (-\sin t\theta \mathbf{u}_1 + \cos t\theta \mathbf{w}_1)}{\text{dist}(\mathbf{x}, L(t))} \right| \\ &\leq 2\theta \left\| \frac{P_{L(t)} \mathbf{x} \mathbf{x}^T P_{L(t)^\perp}}{\text{dist}(\mathbf{x}, L(t))} \right\|. \end{aligned} \quad (35)$$

Now let  $\mathbf{u}_1, \mathbf{u}_2, \dots, \mathbf{u}_d$  and  $\mathbf{v}_1, \mathbf{v}_2, \dots, \mathbf{v}_d$  be the principal vectors between  $L_\star$  and  $L$  with principal angles  $\theta_1, \dots, \theta_d$ , and define that for all  $1 \leq k \leq d$ ,

$$L^{(k)} = \text{Span}(\mathbf{v}_1, \dots, \mathbf{v}_k, \mathbf{u}_{k+1}, \dots, \mathbf{u}_d).$$

In particular,  $L^{(0)} = L_\star$  and  $L^{(d)} = L$ . Then  $\text{dist}(L^{(k-1)}, L^{(k)}) = \theta_k$  and integrating (35) implies that

$$\left| \sum_{\mathbf{x} \in \mathcal{X}_{\text{out}}} \text{dist}(\mathbf{x}, L^{(k)}) - \text{dist}(\mathbf{x}, L^{(k-1)}) \right| \leq \theta_k S_{\text{out}}.$$

Combining the above inequality for all  $0 \leq k \leq d-1$ , (34) is proved.

Then the lemma follows from (33) and (34).  $\square$

*Proof of Lemma 5.* Note that  $\frac{F_{\text{in}}(L)}{|\mathcal{X}_{\text{in}}|} = \text{mean}_{\mathbf{x} \in \mathcal{X}_{\text{in}}} \text{dist}(\mathbf{x}, L)$ , and since  $\text{dist}(\mathbf{x}, L) \leq \sin \theta_1(L, L_\star) \|\mathbf{x}\|$ ,

$$\text{mean}_{\mathbf{x} \in \mathcal{X}_{\text{in}}} \text{dist}(\mathbf{x}, L) \leq \sin \theta_1(L, L_\star) \text{mean}_{\mathbf{x} \in \mathcal{X}_{\text{in}}} \|\mathbf{x}\|.$$

Thus it is sufficient to choose  $c_3$  such that

$$c_3 \sin \theta_1(L, L_\star) \text{mean}_{\mathbf{x} \in \mathcal{X}_{\text{in}}} \|\mathbf{x}\| \leq q_\gamma(\{\text{dist}(\mathbf{x}, L)\}_{\mathbf{x} \in \mathcal{X}}).$$

It is sufficient to prove that there is a  $c_3 > 0$  such that

$$\sup_{L \in \mathcal{G}(D, d)} \frac{|\{\mathbf{x} \in \mathcal{X} : \text{dist}(\mathbf{x}, L) < c_3 \sin \theta_1(L, L_\star) \text{mean}_{\mathbf{x} \in \mathcal{X}_{\text{in}}} \|\mathbf{x}\|\}|}{|\mathcal{X}|} < \gamma, \quad (36)$$

since then the result follows from the definition of  $q_\gamma$ .

We show that Assumption 1 implies that

$$\frac{q_\gamma(\{\text{dist}(\mathbf{x}, L)\}_{\mathbf{x} \in \mathcal{X}})}{\sin \theta_1(L, L_\star)} \quad (37)$$

is uniformly lower bounded by a positive constant for  $L \neq L_\star$ .

First, note that as  $L \rightarrow L_\star$ ,

$$q_\gamma(\{\text{dist}(\mathbf{x}, L)\}_{\mathbf{x} \in \mathcal{X}}) \asymp q_{\gamma \frac{|\mathcal{X}|}{|\mathcal{X}_{\text{in}}|}}(\{\text{dist}(\mathbf{x}, L)\}_{\mathbf{x} \in \mathcal{X}_{\text{in}}}).$$

so that in a neighborhood around  $L_\star$ , we only need to understand the behavior of (37) with respect to the inlier points.

Note that for  $\mathbf{x} \in L_\star$ ,  $\frac{\text{dist}(\mathbf{x}, L)^2}{\sin^2 \theta_1(L, L_\star)} = |\mathbf{x}^T \mathbf{v}_j(L, L_\star)|^2 + \sum_{j=2}^d \frac{\sin^2 \theta_j(L, L_\star)}{\sin^2(\theta_1(L, L_\star))} |\mathbf{x}^T \mathbf{v}_j(L, L_\star)|^2$ , where  $\mathbf{v}_j(L, L_\star)$  is a principal vector for  $L_\star$  relative to  $L$ . We have

$$\begin{aligned} & \{\mathbf{x} \in \mathcal{X}_{\text{in}} : \text{dist}(\mathbf{x}, L) < c_3 \sin \theta_1(L, L_\star) \text{mean}_{\mathbf{x} \in \mathcal{X}_{\text{in}}} \|\mathbf{x}\|\} \\ & \subseteq \{\mathbf{x} \in \mathcal{X}_{\text{in}} : |\mathbf{x}^T \mathbf{v}_1(L, L_\star)| < c_3 \text{mean}_{\mathbf{x} \in \mathcal{X}_{\text{in}}} \|\mathbf{x}\|\}. \end{aligned}$$

By Assumption 1, we thus know that there is a  $c_3$  such that  $\frac{q_\gamma(\{\text{dist}(\mathbf{x}, L)\}_{\mathbf{x} \in \mathcal{X}})}{\sin \theta_1(L, L_\star)} > c_3$  for all  $L \in B(L_\star, \delta)$ .

Define  $L_0 = \text{Sp}(\mathbf{v}_2, \dots, \mathbf{v}_d)$ . Then, by Assumption 1, we know that less than a  $\gamma$  fraction of points lie in  $L_0 \cup L$ . In particular, for  $L \neq L_\star$ ,

$$\frac{q_\gamma(\{\text{dist}(\mathbf{x}, L)\}_{\mathbf{x} \in \mathcal{X}})}{\sin \theta_1(L, L_\star)} > \min(\{|\mathbf{v}_1^T \mathbf{x}| : \mathbf{x} \in \mathcal{X}_{\text{in}} \setminus L_0\} \cup \{\frac{\text{dist}(\mathbf{x}, L)}{\sin \theta_1(L, L_\star)} : \mathbf{x} \in \mathcal{X}_{\text{out}} \setminus L\})$$

Since  $\frac{q_\gamma(\{\text{dist}(\mathbf{x}, L)\}_{\mathbf{x} \in \mathcal{X}})}{\sin \theta_1(L, L_\star)} \not\rightarrow 0$  as  $L \rightarrow L_\star$  and  $\frac{q_\gamma(\{\text{dist}(\mathbf{x}, L)\}_{\mathbf{x} \in \mathcal{X}})}{\sin \theta_1(L, L_\star)}$ , there exists a  $c_3$  such that the Lemma holds. □

## 6.2. Proof of Theorem 2

We begin with some background before proceeding to the proof of the theorem.

### 6.2.1. Background of proof

**A parametrization of paths in  $\mathcal{A}(D, d)$ .** Recall that the underlying affine subspace in our model is  $[A_\star] = [(L_\star, 0)]$ , where we choose the representative  $(L_\star, 0)$  WLOG.

For another affine subspace parametrized by  $A = (L, \mathbf{m})$ , let us consider a path between  $A_\star$  and  $A$  defined as follows: let the principal vectors of  $L_\star$  and  $L$  be

$$L_\star = \text{Sp}(\mathbf{u}_1, \dots, \mathbf{u}_d), \quad L = \text{Sp}(\mathbf{v}_1, \dots, \mathbf{v}_d),$$

where  $\mathbf{v}_i = \cos \theta_i \mathbf{u}_i + \sin \theta_i \mathbf{w}_i$  such that  $\mathbf{u}_i \perp \mathbf{w}_j$  for all  $1 \leq i, j \leq d$ .



Then a path of affine subspaces from  $A_\star$  to  $A$  given by  $C : [0, 1] \rightarrow \mathcal{A}(D, d)$  is defined by

$$C(t) = (1-t)\mathbf{a}_\star + t\mathbf{a} + \text{Sp}(\{\cos t\theta_i \mathbf{u}_i + \sin t\theta_i \mathbf{w}_i\}_{i=1}^d), \quad (38)$$

where  $\mathbf{a}_\star$  is the point in  $A_\star$  closest to  $A$  and  $\mathbf{a}$  is the point on  $A$  closest to  $A_\star$ . Note that we have  $\mathbf{a} - \mathbf{a}_\star \perp \text{Sp}(L \oplus L_\star)$ . Denote  $\mathbf{b} = \mathbf{a} - \mathbf{a}_\star$ , then

$$C(t) = \mathbf{a}_\star + t\mathbf{b} + \text{Sp}(\{\cos t\theta_i \mathbf{u}_i + \sin t\theta_i \mathbf{w}_i\}_{i=1}^d). \quad (39)$$

Note that here

$$\text{dist}^2(0, A) = \text{dist}^2(-\mathbf{a}, L) = \text{dist}^2(-\mathbf{a}_\star - \mathbf{b}, L) \quad (40)$$

$$\begin{aligned} &= \|\mathbf{b}\|^2 + \sum_{i=1}^d \text{dist}^2(-\mathbf{P}_{\text{Sp}(\mathbf{u}_i, \mathbf{w}_i)} \mathbf{a}_\star, \text{Sp}(\{\cos \theta_i \mathbf{u}_i + \sin \theta_i \mathbf{w}_i\}_{i=1}^d)) \\ &= \|\mathbf{b}\|^2 + \sum_{i=1}^d (\mathbf{a}_\star^T \mathbf{u}_i)^2 \sin^2 \theta_i \end{aligned} \quad (41)$$

where the last step applies that  $\mathbf{a}_\star \perp \mathbf{w}_i$ . Therefore the definition in Section 4.2 gives

$$\begin{aligned} \text{dist}^2(A_\star, [A]) &= \text{dist}^2(0, [A]) + \sum_j \theta_j^2 \\ &= \|\mathbf{b}\|^2 + \sum_{i=1}^d ((\mathbf{a}_\star^T \mathbf{u}_i)^2 \sin^2 \theta_i + \theta_i^2). \end{aligned} \quad (42)$$

**Auxiliary functions** Similar to the proof of Theorem 1, the proof of Theorem 2 also depends on  $F_\epsilon^{(a)}(A)$ , a regularized objective function  $F^{(a)}$  defined in (10):

$$F_\epsilon^{(a)}(A) = \sum_{\mathbf{x} \in \mathcal{X}: \text{dist}(\mathbf{x}, A) > \epsilon} \text{dist}(\mathbf{x}, A) + \sum_{\mathbf{x} \in \mathcal{X}: \text{dist}(\mathbf{x}, A) \leq \epsilon} \left( \frac{1}{2}\epsilon + \frac{\text{dist}(\mathbf{x}, A)^2}{2\epsilon} \right). \quad (43)$$

Define

$$\begin{aligned} G_{\epsilon_k}^{(a)}(A, A_0) &= \sum_{\mathbf{x} \in \mathcal{X}: \text{dist}(\mathbf{x}, A_0) > \epsilon_k} \left( \frac{1}{2} \text{dist}(\mathbf{x}_i, A_0) + \frac{\text{dist}(\mathbf{x}_i, A)^2}{2 \text{dist}(\mathbf{x}_i, A_0)} \right) + \\ &\quad \sum_{\mathbf{x} \in \mathcal{X}: \text{dist}(\mathbf{x}, A_0) \leq \epsilon_k} \left( \frac{1}{2} \epsilon_k + \frac{\text{dist}(\mathbf{x}_i, A)^2}{2\epsilon} \right). \end{aligned} \quad (44)$$

### 6.2.2. Proof of Theorem 2

We prove that the algorithm ensures the sequence  $F_{\epsilon_k}^{(a)}(A^{(k)})$  is nonincreasing over iterations. That is, we aim to generalize Lemma 2 to the affine setting.

**Lemma 7** (Decrease over iterations, affine case).

$$F_\epsilon(A) - F_\epsilon(T^{(a)}(A)) \geq c\epsilon \text{dist}(A_\star, [A]). \quad (45)$$

*Proof of Lemma 7.* Let us first investigate  $\text{dist}^2(\mathbf{x}, C(t))$ . Since  $C(t)$  defined in (38) can be decomposed into the direct sum of  $d + 1$  components (note that by definition,  $\mathbf{P}_{\text{Sp}(L \oplus L_\star)} \mathbf{a} = \mathbf{P}_{\text{Sp}(L \oplus L_\star)} \mathbf{a}_\star$ ):

$$\mathbf{P}_{\text{Sp}(\mathbf{u}_i, \mathbf{w}_i)} C(t) = (\mathbf{u}_i \mathbf{u}_i^T + \mathbf{w}_i \mathbf{w}_i^T) \mathbf{a}_\star + \text{Sp}(\cos t\theta_i \mathbf{u}_i + \sin t\theta_i \mathbf{w}_i), 1 \leq i \leq d \quad (46)$$

$$\mathbf{P}_{\text{Sp}(L \oplus L_\star)^\perp} C(t) = t\mathbf{b}, \quad (47)$$

the distances  $\text{dist}^2(\mathbf{x}, C(t))$  can also be decomposed using

$$\begin{aligned} & \text{dist}^2(\mathbf{x}, C(t)) \\ &= \|\mathbf{P}_{\text{Sp}(L \oplus L_\star)^\perp} \mathbf{x} - t\mathbf{b}\|^2 + \sum_{i=1}^d \text{dist}^2(\mathbf{P}_{\text{Sp}(\mathbf{u}_i, \mathbf{w}_i)} \mathbf{x}, \mathbf{P}_{\text{Sp}(\mathbf{u}_i, \mathbf{w}_i)} C(t)) \\ &= \|\mathbf{P}_{\text{Sp}(L \oplus L_\star)^\perp} \mathbf{x} - t\mathbf{b}\|^2 + \sum_{i=1}^d ((\mathbf{u}_i \sin t\theta_i - \mathbf{w}_i \cos t\theta_i)^T (\mathbf{x} - (\mathbf{u}_i \mathbf{u}_i^T + \mathbf{w}_i \mathbf{w}_i^T) \mathbf{a}_\star))^2 \\ &= \|\mathbf{P}_{\text{Sp}(L \oplus L_\star)^\perp} \mathbf{x} - t\mathbf{b}\|^2 + \sum_{i=1}^d ((\mathbf{x} - \mathbf{a}_\star)^T \mathbf{u}_i \sin t\theta_i - \mathbf{x}^T \mathbf{w}_i \cos t\theta_i)^2, \end{aligned}$$

where the last step follows from  $\mathbf{w}_i \perp L_\star$  and  $\mathbf{a}_\star \in L_\star$ . Note also that  $(\mathbf{x} - \mathbf{a}_\star)^T \mathbf{u}_i \sin t\theta_i - \mathbf{x}^T \mathbf{w}_i \cos t\theta_i = \sin(t\theta_i - \theta'_i) \sqrt{((\mathbf{x} - \mathbf{a}_\star)^T \mathbf{u}_i)^2 + (\mathbf{x}^T \mathbf{w}_i)^2}$  for some  $\theta'_i$

We proceed by studying  $\varphi(t) = G_\epsilon^{(a)}(C(t), A)$ . In particular, we will bound the first and second derivatives of  $\varphi$ . Since the second derivative of  $\sin^2 x$  is bounded in  $[-2, 2]$ , we have

$$\begin{aligned} \frac{d^2}{dt^2} \text{dist}^2(\mathbf{x}, C(t)) &\leq 2\|\mathbf{b}\|^2 + 2 \sum_{i=1}^d \theta_i^2 \left[ ((\mathbf{x} - \mathbf{a}_\star)^T \mathbf{u}_i)^2 + (\mathbf{x}^T \mathbf{w}_i)^2 \right] \\ &\leq 2\|\mathbf{b}\|^2 + 2\theta_1^2 \|\mathbf{x} - \mathbf{a}_\star\|^2 \leq 2\|\mathbf{b}\|^2 + 4\theta_1^2 (\|\mathbf{x}\|^2 + \|\mathbf{a}_\star\|^2) \leq \dots \\ &\leq 2\|\mathbf{b}\|^2 + 2 \sum_{i=1}^d \theta_i^2 [2(\mathbf{a}_\star^T \mathbf{u}_i)^2 + 2(\mathbf{x}^T \mathbf{u}_i)^2 + (\mathbf{x}^T \mathbf{w}_i)^2] \\ &\leq 4\|\mathbf{x}\|^2 \sum_{i=1}^n \theta_i^2 + 10 \text{dist}^2(0, [A]) \\ &= 10 \max(\|\mathbf{x}\|^2, 1) \text{dist}^2(A_\star, [A]), \end{aligned}$$

where the last two steps apply (40) and  $\theta \leq \pi \sin \theta/2$ .

Combining the above estimation for all  $\mathbf{x} \in \mathcal{X}$ , we have

$$\varphi''(t) = \frac{d^2}{dt^2} G_\epsilon^{(a)}(C(t), A) \leq \frac{C}{\epsilon} \text{dist}^2(A_\star, [A])$$

for some  $C$  depending on  $\mathcal{X}$ .

As for the first derivative of  $\text{dist}^2(\mathbf{x}, C(t))$  at  $t = 1$ , we have

$$\begin{aligned} \frac{d}{dt} \text{dist}^2(\mathbf{x}, C(t)) \Big|_{t=1} &= \mathbf{b}^T (\mathbf{P}_{\text{Sp}(L \oplus L_\star)^\perp} \mathbf{x} - \mathbf{b}) \\ &+ \sum_{i=1}^d \theta_i \left( (\mathbf{x} - \mathbf{a}_\star)^T \mathbf{u}_i \sin \theta_i - \mathbf{x}^T \mathbf{w}_i \cos \theta_i \right) \left( (\mathbf{x} - \mathbf{a}_\star)^T \mathbf{u}_i \cos \theta_i + \mathbf{x}^T \mathbf{w}_i \sin \theta_i \right). \end{aligned}$$

Combining it with

$$\text{dist}(\mathbf{x}, C(1)) = \sqrt{\left\| \mathbf{P}_{\text{Sp}(L \oplus L_\star)^\perp} \mathbf{x} - \mathbf{b} \right\|^2 + \sum_{i=1}^d \left( (\mathbf{x} - \mathbf{a}_\star)^T \mathbf{u}_i \sin \theta_i - \mathbf{x}^T \mathbf{w}_i \cos \theta_i \right)^2},$$

we have

$$\begin{aligned} \frac{\frac{d}{dt} \text{dist}^2(\mathbf{x}, C(t)) \Big|_{t=1}}{\text{dist}(\mathbf{x}, C(1))} &\leq \sqrt{\left\| \mathbf{b} \right\|^2 + \sum_{i=1}^d \theta_i^2 \left( (\mathbf{x} - \mathbf{a}_\star)^T \mathbf{u}_i \cos \theta_i + \mathbf{x}^T \mathbf{w}_i \sin \theta_i \right)^2} \\ &\leq \sqrt{\left\| \mathbf{b} \right\|^2 + \sum_{i=1}^d \theta_i^2 \left( (\mathbf{x} - \mathbf{a}_\star)^T \mathbf{u}_i \right)^2} + \sqrt{\sum_{i=1}^d \theta_i^4 (\mathbf{x}^T \mathbf{w}_i)^2} \\ &\leq \frac{\pi}{2} \text{dist}(\mathbf{P}_{A_\star} \mathbf{x}, [A]) + \sum_{i=1}^d \theta_i^2 (\mathbf{x}^T \mathbf{w}_i)^2. \end{aligned}$$

On the other hand, if we restrict that  $\mathbf{x} \in \mathcal{X}_{\text{in}}$ , then

$$\begin{aligned} \text{dist}^2(\mathbf{x}, C(1)) &= \text{dist}^2(\mathbf{x}, [A]) = \left\| \mathbf{b} \right\|^2 + \sum_{i=1}^d \left( (\mathbf{x} - \mathbf{a}_\star)^T \mathbf{u}_i \right)^2 \sin^2 \theta_i \\ \frac{d}{dt} \text{dist}^2(\mathbf{x}, C(t)) \Big|_{t=1} &= \left\| \mathbf{b} \right\|^2 + \sum_{i=1}^d \theta_i \left( (\mathbf{x} - \mathbf{a}_\star)^T \mathbf{u}_i \right)^2 \sin \theta_i \cos \theta_i \geq \cos^2 \theta_1 \text{dist}^2(\mathbf{x}, C(1)). \end{aligned}$$

Combining the estimations above, along with

$$\sum_{\mathbf{x} \in \mathcal{X}} \sum_{i=1}^d \theta_i^2 (\mathbf{x}^T \mathbf{w}_i)^2 \leq \sum_{i=1}^d \theta_i^2 \left\| \mathbf{P}_{L_\star^\perp} \mathbf{X}_{\text{out}} \right\|^2,$$

we have that for  $\varphi(t) = G_\epsilon^{(a)}(C(t), A)$ ,

$$\varphi'(1) \geq \sum_{\mathbf{x} \in \mathcal{X}_{\text{in}}} \frac{\cos^2 \theta_1 \text{dist}^2(\mathbf{x}, A)}{2 \max(\text{dist}(\mathbf{x}, A), \epsilon)} - \sum_{\mathbf{x} \in \mathcal{X}_{\text{out}}} \left( \frac{\pi}{2} \text{dist}(\mathbf{P}_{A_\star} \mathbf{x}, [A]) + \theta_1^2 \left\| \mathbf{P}_{L_\star^\perp} \mathbf{x} \right\|^2 \right).$$

Recall from definition of  $F, G$ , we have

$$\min_t \varphi(t) \geq G_\epsilon(T^{(a)}(A), A) \geq F_\epsilon(T^{(a)}(A)),$$

and combining it with Assumption 4 and the estimation of  $\varphi''(t)$  and  $\varphi'(1)$  above, we have

$$F_\epsilon(A) - F_\epsilon(T^{(a)}(A)) \geq \varphi(1) - \min_t \varphi(t) \geq \frac{(\varphi'(1))^2}{2 \max_t \varphi''(t)} \geq c\epsilon \text{dist}(A_\star, [A]),$$

and the Lemma is proved.  $\square$

The following lemma generalizes Lemma 5 and the proof is similar.

**Lemma 8.** *Under Assumption 3, there exists  $c_3 > 0$  such that for all  $[A] \in \mathcal{A}(D, d)$ ,*

$$q_\gamma(\{\text{dist}(\mathbf{x}, [A])\}_{\mathbf{x} \in \mathcal{X}}) \geq c_3 \frac{F_{\text{in}}^{(a)}(A)}{|\mathcal{X}_{\text{in}}|}. \quad (48)$$

The next lemma shows that  $\text{dist}(A_\star, [A])$  serves as a lower bound for the FMS objective over at least half of the inliers:

**Lemma 9.** *Under Assumption 3, for any subset  $\mathcal{X}'_{\text{in}} \subseteq \mathcal{X}_{\text{in}}$  with  $|\mathcal{X}'_{\text{in}}| \geq \frac{1}{2}|\mathcal{X}_{\text{in}}|$ , we have*

$$\sum_{\mathbf{x} \in \mathcal{X}'_{\text{in}}} \text{dist}(\mathbf{x}, A) \geq c \cdot \text{dist}(A_\star, [A]), \quad (49)$$

for some constant  $c > 0$ .

*Proof of Lemma 9.* Let  $\mathbf{b}$  denote the projection of the origin onto the affine subspace  $A_\star$ . For each inlier  $\mathbf{x} \in A_\star$ , we can express

$$\mathbf{x} = \sum_{j=1}^d a_j \mathbf{v}_j + \mathbf{b},$$

where  $\{\mathbf{v}_j\}_{j=1}^d$  form an orthonormal basis for the linear part of  $A_\star$ . Let  $\{\mathbf{u}_j\}_{j=1}^d$  and  $\{\mathbf{w}_j\}_{j=1}^d$  be orthonormal vectors such that each  $\mathbf{u}_j$  can be decomposed as

$$\mathbf{u}_j = \cos \theta_j \mathbf{v}_j + \sin \theta_j \mathbf{w}_j,$$

with  $\mathbf{w}_j \perp A_\star$ . Then the squared distance from  $\mathbf{x}$  to  $A$  can be written as

$$\text{dist}(\mathbf{x}, A)^2 = \sum_{j=1}^d \left( \sin \theta_j \cdot \mathbf{x}^\top \mathbf{u}_j + \mathbf{b}^\top \mathbf{w}_j \right)^2.$$

Note that the distance from  $A_\star$  to  $[A]$  satisfies

$$\text{dist}(A_\star, [A])^2 = \|\mathbf{b}\|^2 + \sum_{j=1}^d \theta_j^2.$$

Now suppose, for contradiction, that the claim does not hold. Then there exists an affine subspace  $A \neq A_\star$  such that  $\text{dist}(A_\star, [A]) \neq 0$ , yet

$$\sum_{\mathbf{x} \in \mathcal{X}'_{\text{in}}} \text{dist}(\mathbf{x}, A) = 0.$$

This implies that all points in  $\mathcal{X}'_{\text{in}}$  lie entirely within  $A$ , contradicting Assumption 3, which asserts that any affine subspace distinct from  $A_\star$  cannot contain more than half of the inliers.

Therefore, the bound (49) must hold for some constant  $c > 0$ , completing the proof.  $\square$

*Proof of Theorem 2.* The proof of Theorem 2 follows similarly from the proof of Theorem 1. In particular, Lemma 7 implies that

$$F_{\epsilon_k}^{(a)}(A^{(k)}) - F_{\epsilon_k}^{(a)}(T^{(a)}(A^{(k+1)})) \geq C\epsilon_k.$$

On the other hand, use the same argument as in Lemma 4(a), we have

$$F_{in, \epsilon_k}^{(a)}(A^{(k)}) \leq 2F_{in}^{(a)}(A_\star)$$

and the argument in Lemma 7 implies that

$$|F_{out, \epsilon_k}^{(a)}(A^{(k)}) - F_{out, \epsilon_k}^{(a)}(A_\star)| \leq F_{in}^{(a)}(A^{(k)})/2.$$

In summary,

$$F_{\epsilon_k}^{(a)}(A^{(k)}) - F^{(a)}(A_\star) \leq 3F_{in}^{(a)}(A^{(k)}).$$

Combining it with

$$\begin{aligned} F_{in}^{(a)}(A^{(k)}) &= \sum_{\mathbf{x} \in \mathcal{X}_{in}} \text{dist}(\mathbf{x}, A^{(k)}) \\ &\leq \sum_{\mathbf{x} \in \mathcal{X}_{in}} \text{dist}(\mathbf{x}, L^{(k)}) + \text{dist}(A_\star, [A^{(k)}]) \\ &\leq \text{dist}(A_\star, [A^{(k)}]) \sum_{\mathbf{x} \in \mathcal{X}_{in}} (\|\mathbf{x}\| + 1) \end{aligned}$$

and Lemma 8, the same argument as in Theorem 1 can be applied to prove the convergence.  $\square$

### 6.3. Proof of Proposition 2

The following lemma gives bounds on the statistics  $S_{in}$  and  $S_{out}$  defined in (11) under this model with high probability. From the lemma proved here, the proof of Proposition 2 follows.

**Lemma 10** (Estimation of parameters under the Haystack model). *Assuming that  $n = O(D^3 \log D)$ ,  $\epsilon \leq 1$ , and  $d \leq D - 2$ , then we have the following estimations of parameters in Theorems 1 and Assumption 2: with high probability,*

$$S_{in} > Cn_{in}\sigma_{in}/\sqrt{d}, \quad S_{out} \leq C \frac{n_{out}\sigma_{out}}{\sqrt{D(D-d)}}, \quad \sigma_d \left( \sum_{\mathbf{x} \in \mathcal{X}_{in}} \frac{\mathbf{x}\mathbf{x}^T}{\max(\|\mathbf{x}\|, \epsilon)} \right) \geq Cn_{in}\sigma_{in}/d.$$

*Proof.* For  $S_{in}$ , it follows from (Lerman et al., 2015, Lemma 8.2) that

$$\Pr \left( S_{in} \geq \left( \sqrt{\frac{\pi}{2}} n_{in} - 2\sqrt{n_{in}d} - t\sqrt{n_{in}} \right) \sigma_d(\Sigma_{in}) \right) \geq 1 - e^{-t^2/2}$$

On the other hand we can use (Maunu et al., 2019, Proposition 12) to show that

$$\Pr \left( \sigma_d \left( \sum_{\mathbf{x} \in \mathcal{X}_{in}} \frac{\mathbf{x}\mathbf{x}^T}{\max(\|\mathbf{x}\|, \epsilon)} \right) \geq \frac{\lambda_d(\Sigma_{in})}{\lambda_1(\Sigma_{in})^{1/2}} \frac{(1-a)^2 N_{in}}{d} + O \left( \sqrt{\frac{N_{in}}{d}} \right) \right) \geq 1 - 4e^{-c_1 a^2 N_{in}}.$$

For  $S_{out} \leq \max_{L \in \mathcal{G}(D, d)} \left\| \sum_{\mathbf{x} \in \mathcal{S}_{out}} \frac{\mathbf{x}\mathbf{x}^T \mathbf{P}_{L^\perp}}{\text{dist}(\mathbf{x}, L)} \right\|$ , we first prove its bound for any fixed  $L$  and then apply a,  $\epsilon$ -net argument.

**Estimation for fixed  $L \in G(D, d)$ :** Assuming that  $|\mathcal{X}_{\text{out}}| = n_0$ , then Lerman et al. (2015, Proposition 8.3, Lemma 8.4) proved that with probability at least  $1 - e^{t_1^2/2} - 1.5e^{t_2^2/2}$ ,

$$\|\mathbf{P}_L \mathbf{X}\| \geq \sigma_{\text{out}}(\sqrt{d} + \sqrt{n_0} + t_1)/\sqrt{D},$$

and for  $\mathbf{S}$ , a  $n_0 \times D$  matrix with each row given by  $\mathbf{P}_{L^\perp} \mathbf{x} / \|\text{dist}(\mathbf{x}, L)\|$ ,

$$\|\mathbf{S}\| \geq C \frac{\sqrt{D-d} + \sqrt{n_0} + t_2}{\sqrt{D-d-0.5}}.$$

As a result, with probability at least  $1 - e^{t_1^2/2} - 1.5e^{t_2^2/2}$  we have

$$\left\| \sum_{\mathbf{x} \in \mathcal{S}_{\text{out}}} \frac{\mathbf{x} \mathbf{x}^T \mathbf{P}_{L^\perp}}{\text{dist}(\mathbf{x}, L)} \right\| \geq C \sigma_{\text{out}} \frac{\sqrt{D-d} + \sqrt{n_0} + t_2}{\sqrt{D-d-0.5}} \frac{\sqrt{d} + 2\sqrt{n_0} + t_1}{\sqrt{D}}. \quad (50)$$

**Covering argument:** And for any  $L_1, L_2 \in \mathcal{G}(D, d)$ , applying

$$\left\| \frac{\mathbf{P}_{L_1^\perp} \mathbf{x}}{\text{dist}(\mathbf{x}, L_1)} - \frac{\mathbf{P}_{L_2^\perp} \mathbf{x}}{\text{dist}(\mathbf{x}, L_2)} \right\| < 2 \min \left( \frac{\|\mathbf{P}_{L_1^\perp} - \mathbf{P}_{L_2^\perp}\| \|\mathbf{x}\|}{\text{dist}(\mathbf{x}, L_1)}, 1 \right),$$

we have

$$\left\| \sum_{\mathbf{x} \in \mathcal{S}_{\text{out}}} \frac{\mathbf{P}_{L_1} \mathbf{x} \mathbf{x}^T \mathbf{P}_{L_1^\perp}}{\text{dist}(\mathbf{x}, L_1)} - \sum_{\mathbf{x} \in \mathcal{S}_{\text{out}}} \frac{\mathbf{P}_{L_2} \mathbf{x} \mathbf{x}^T \mathbf{P}_{L_2^\perp}}{\text{dist}(\mathbf{x}, L_2)} \right\| \leq \sum_{\mathbf{x} \in \mathcal{S}_{\text{out}}} \|\mathbf{x}\| 2 \min \left( \frac{\|\mathbf{P}_{L_1^\perp} - \mathbf{P}_{L_2^\perp}\| \|\mathbf{x}\|}{\text{dist}(\mathbf{x}, L_1)}, 1 \right). \quad (51)$$

When  $d \leq D - 2$ , then  $\|\mathbf{x}\| 2 \min \left( \frac{\|\mathbf{P}_{L_1^\perp} - \mathbf{P}_{L_2^\perp}\| \|\mathbf{x}\|}{\text{dist}(\mathbf{x}, L_1)}, 1 \right)$  has expectation bounded by  $C \sigma_{\text{out}} \|\mathbf{P}_{L_1^\perp} - \mathbf{P}_{L_2^\perp}\| \sqrt{D/(D-d)}$ . So Hoeffding's inequality in Theorem 2.6.2 of Vershynin (2018) implies that the RHS of (51) is close to its expectation and with high probability that, it is bounded above by

$$C n_0 \sigma_{\text{out}} \|\mathbf{P}_{L_1^\perp} - \mathbf{P}_{L_2^\perp}\| \sqrt{D/(D-d)}.$$

Combining it with a epsilon-net covering argument over  $L \in \mathcal{G}(D, d)$ , the estimation of  $\mathcal{S}_{\text{out}}$  for a fixed  $L$  in (50), and  $n_0 \approx \alpha_0 n$ , we have the estimation of  $\mathcal{S}_{\text{out}}$  in Lemma 10.  $\square$

#### 6.4. Proof of Propositions 3 and 4

*Proof of Proposition 3.* Let  $a = \text{dist}(0, [A])$ , where  $[A] = [(L, \mathbf{m})]$ , and denote the largest principal angle between  $L$  and  $L_\star$  by  $\theta_1$ . Then,

$$\frac{1}{n} \sum_{\mathbf{x} \in \mathcal{X}_{\text{in}}} \|\mathbf{Q}_L \mathbf{x}\| = \frac{1}{n} \sum_{\mathbf{x} \in \mathcal{X}_{\text{in}}} \sin(\angle(\mathbf{x}, L)) \|\mathbf{x}\| \leq \frac{1}{n} \sum_{\mathbf{x} \in \mathcal{X}_{\text{in}}} \theta_1 \|\mathbf{x}\| \xrightarrow{n \rightarrow \infty} O\left(\frac{\alpha_{\text{in}} \theta_1}{\sqrt{d}}\right).$$

Thus,

$$\begin{aligned} \frac{1}{n} \sum_{\mathbf{x} \in \mathcal{X}'_{\text{in}}} \text{dist}(\mathbf{x}, [A]) &= \frac{1}{n} \sum_{\mathbf{x} \in \mathcal{X}'_{\text{in}}} \|\mathbf{Q}_L(\mathbf{x} - \mathbf{m})\| \\ &\leq \frac{1}{n} \sum_{\mathbf{x} \in \mathcal{X}'_{\text{in}}} \|\mathbf{Q}_L \mathbf{x}\| + \frac{1}{n} \sum_{\mathbf{x} \in \mathcal{X}'_{\text{in}}} \|\mathbf{Q}_L \mathbf{m}\| \\ &= O\left(\alpha_{\text{in}} \left(\frac{\theta_1}{\sqrt{d}} + a\right)\right). \end{aligned} \quad (52)$$

On the other hand, for any  $\mathbf{x}$ , we have

$$\text{dist}(P_{A_*} \mathbf{x}, [A]) \leq \text{dist}(P_{A_*} \mathbf{x}, L) + a \leq O(\theta_1 \|P_{A_*} \mathbf{x}\| + a).$$

As a result, the following inequality

$$\frac{1}{\cos^2 c_0} \sum_{\mathbf{x} \in \mathcal{X}'_{\text{in}}} \text{dist}(\mathbf{x}, A) \geq 4 \cdot \frac{\pi}{2} \sum_{\mathbf{x} \in \mathcal{X}_{\text{out}}} \text{dist}(P_{A_*} \mathbf{x}, [A])$$

holds when

$$\frac{\alpha_{\text{in}}}{\alpha_{\text{out}}} \geq O\left(\max\left(\sqrt{d} \int_{\mathbf{x} \sim \mu_{\text{out}}} \|P_{A_*} \mathbf{x}\|, 1\right)\right).$$

Furthermore, applying (52) again, we also obtain the following inequality

$$\frac{1}{\cos^2 c_0} \sum_{\mathbf{x} \in \mathcal{X}'_{\text{in}}} \text{dist}(\mathbf{x}, A) \geq 4 \cdot \theta_1(L, L_*)^2 \left\| P_{L_*^\perp} \left( \sum_{\mathbf{x} \in \mathcal{X}_{\text{out}}} \mathbf{x} \mathbf{x}^\top \right) P_{L_*^\perp} \right\|$$

under the condition:

$$\frac{\alpha_{\text{in}}}{\alpha_{\text{out}}} \geq \theta_1(L, L_*)^2 \cos^2 c_0 \cdot \sqrt{d} \left\| \int_{\mathbf{x} \sim \mu_{\text{out}}} P_{L_*^\perp} \mathbf{x} \mathbf{x}^\top P_{L_*^\perp} d\mathbf{x} \right\|,$$

when  $\theta_1(L, L_*) \leq c_0$ .

Combining the estimations above, the proposition is proved.  $\square$

*Proof of Proposition 4.* Recall that the inliers are distributed as  $\mathcal{N}(0, \Sigma_{\text{in}}/d)$ , while the projected outliers  $P_{A_*} \mathbf{x}$  follow the distribution  $\mathcal{N}(0, \mathbf{P}_{L_*} \Sigma_{\text{out}} \mathbf{P}_{L_*} / D)$ .

Since the function  $\text{dist}(\mathbf{x}, [A])$  is convex in  $\mathbf{x}$ , and using the assumption  $\sigma_d(\Sigma_{\text{in}}) \geq 1$ , we obtain

$$\int_{\mathbf{x} \sim \mu_{\text{in}}} \text{dist}(\mathbf{x}, [A]) \geq \int_{\mathbf{x} \sim \mu_0} \text{dist}(\mathbf{x}, [A]),$$

where  $\mu_0 \sim \mathcal{N}(0, \mathbf{P}_{L_*}/d)$ .

Similarly, since  $\sigma_1(\Sigma_{\text{out}})^2 \leq D/d$ , it follows that

$$\mathbf{P}_{L_*} \Sigma_{\text{out}} \mathbf{P}_{L_*} / D \preceq \mathbf{P}_{L_*} / d,$$

and thus

$$\int_{\mathbf{x} \sim \mu_0} \text{dist}(\mathbf{x}, [A]) \geq \int_{\mathbf{x} \sim \mu_{\text{out}}} \text{dist}(P_{A_*} \mathbf{x}, [A]).$$

Additionally, observe that

$$\left\| \int_{\mathbf{x} \sim \mu_{\text{out}}} P_{L_*^\perp} \mathbf{x} \mathbf{x}^\top P_{L_*^\perp} d\mathbf{x} \right\| \leq \frac{\|\Sigma_{\text{out}}\|^2}{D} \leq \frac{\sigma_{\text{out}}^2}{D}.$$

Combining this bound with the inlier estimation (52) and using the assumption  $\theta_1 \leq c_0$ , the proposition follows.  $\square$

## 7. Conclusion

In this work we have revisited the use of IRLS algorithms for robust subspace recovery. In the case of linear subspaces, which is the FMS algorithm Lerman and Maunu (2018a), we have incorporated dynamic smoothing, which allows us to prove a global recovery result under a deterministic condition. We have extended the FMS algorithm to the affine setting, where we are able to show a local recovery result under a deterministic condition. These results represent significant theoretical contributions: this paper is the first to demonstrate global recovery for a nonconvex IRLS procedure and for IRLS over a Riemannian manifold, and it is the first to include a convergence analysis for an algorithm in affine robust subspace recovery. We include an example application of the (A)FMS algorithms to low-dimensional training of neural networks, where the found subspaces perform better than alternatives like PCA.

There are many open questions for future work. While our results are stable to small perturbations of the inliers, detailed noise analysis in robust subspace recovery is still an open question. In the case of affine subspace recovery, it would be interesting to show if a similar global convergence result holds as in the linear case or if there are some obstructions to such a result. Another avenue is to develop a deeper understanding of how robust subspaces have better generalization in the training of neural networks, and to leverage this in specialized subspace recovery algorithms for this setting.

## 8. Acknowledgements

G. Lerman was supported by the NSF under Award No. 2152766. T. Maunu was supported by the NSF under Award No. 2305315. T. Zhang was supported by the NSF under Award No. 2318926.

## References

- P.-A. Absil, R. Mahony, and R. Sepulchre. *Optimization Algorithms on Matrix Manifolds*. Princeton University Press, USA, 2007. ISBN 0691132984.
- Ery Arias-Castro and Jue Wang. RANSAC algorithms for subspace recovery and subspace clustering. *arXiv preprint*, 2017.
- Gerard Ben Arous, Reza Gheissari, Jiaoyang Huang, and Aukosh Jagannath. High-dimensional SGD aligns with emerging outlier eigenspaces. In *The Twelfth International Conference on Learning Representations*, 2024.
- Ronen Basri and David W Jacobs. Lambertian reflectance and linear subspaces. *IEEE Transactions on Pattern Analysis and Machine Intelligence*, 25(2):218–233, 2003.



- Amir Beck and Israel Rosset. A dynamic smoothing technique for a class of nonsmooth optimization problems on manifolds. *SIAM Journal on Optimization*, 33(3):1473–1493, 2023.
- Amir Beck and Shoham Sabach. Weiszfeld’s method: Old and new results. *Journal of Optimization Theory and Applications*, 164(1):1–40, 2015. doi: 10.1007/s10957-014-0586-7.
- Nicolas Boumal. *An introduction to optimization on smooth manifolds*. Cambridge University Press, 2023.
- Emmanuel J Candès, Xiaodong Li, Yi Ma, and John Wright. Robust principal component analysis? *Journal of the ACM*, 58(3):11, 2011.
- Avishek Chatterjee and Venu Madhav Govindu. Robust relative rotation averaging. *IEEE Transactions on Pattern Analysis and Machine Intelligence*, 40(4):958–972, 2017.
- Shixiang Chen, Zengde Deng, Shiqian Ma, and Anthony Man-Cho So. Manifold proximal point algorithms for dual principal component pursuit and orthogonal dictionary learning. In *2019 53rd Asilomar Conference on Signals, Systems, and Computers*, pages 259–263, 2019.
- Kenneth L. Clarkson and David P. Woodruff. Input sparsity and hardness for robust subspace approximation. In *2015 IEEE 56th Annual Symposium on Foundations of Computer Science*, pages 310–329, 2015.
- Marina Danilova, Pavel Dvurechensky, Alexander Gasnikov, Eduard Gorbunov, Sergey Guminov, Dmitry Kamzolov, and Innokentiy Shibaev. Recent theoretical advances in non-convex optimization. In *High-Dimensional Optimization and Probability: With a View Towards Data Science*, pages 79–163. Springer, 2022.
- Ingrid Daubechies, Ronald DeVore, Massimo Fornasier, and C Sinan Güntürk. Iteratively reweighted least squares minimization for sparse recovery. *Communications on Pure and Applied Mathematics*, 63(1):1–38, 2010.
- Jia Deng, Wei Dong, Richard Socher, Li-Jia Li, Kai Li, and Li Fei-Fei. Imagenet: A large-scale hierarchical image database. In *IEEE Conference on Computer Vision and Pattern Recognition (CVPR)*, pages 248–255, 2009.
- Chris Ding, Ding Zhou, Xiaofeng He, and Hongyuan Zha. R1-pca: rotational invariant L1-norm principal component analysis for robust subspace factorization. In *Proceedings of the 23rd International Conference on Machine Learning*, pages 281–288, 2006.

- Tianjiao Ding, Yunchen Yang, Zhihui Zhu, Daniel P Robinson, René Vidal, Laurent Kneip, and Manolis C Tsakiris. Robust homography estimation via dual principal component pursuit. In *Proceedings of the IEEE/CVF Conference on Computer Vision and Pattern Recognition*, pages 6080–6089, 2020.
- Tianyu Ding, Zhihui Zhu, René Vidal, and Daniel P Robinson. Dual principal component pursuit for robust subspace learning: Theory and algorithms for a holistic approach. In *International Conference on Machine Learning*, pages 2739–2748. PMLR, 2021.
- Tianyu Ding, Jinxin Zhou, Tianyi Chen, Zhihui Zhu, Ilya Zharkov, and Luming Liang. Adacontour: Adaptive contour descriptor with hierarchical representation. *arXiv preprint arXiv:2404.08292*, 2024.
- Alan Edelman, Tomás A Arias, and Steven T Smith. The geometry of algorithms with orthogonality constraints. *SIAM Journal on Matrix Analysis and Applications*, 20(2):303–353, 1998.
- Martin A Fischler and Robert C Bolles. Random sample consensus: a paradigm for model fitting with applications to image analysis and automated cartography. *Communications of the ACM*, 24(6):381–395, 1981.
- Massimo Fornasier, Holger Rauhut, and Rachel Ward. Low-rank matrix recovery via iteratively reweighted least squares minimization. *SIAM Journal on Optimization*, 21(4):1614–1640, 2011.
- Moritz Hardt and Ankur Moitra. Algorithms and hardness for robust subspace recovery. In *Conference on Learning Theory*, pages 354–375. PMLR, 2013.
- Richard Hartley and Andrew Zisserman. *Multiple view geometry in computer vision*. Cambridge University Press, 2003.
- Paul W Holland and Roy E Welsch. Robust regression using iteratively reweighted least-squares. *Communications in Statistics-theory and Methods*, 6(9):813–827, 1977.
- Harold Hotelling. Analysis of a complex of statistical variables into principal components. *Journal of Educational Psychology*, 24(6):417, 1933.
- Jiang Hu, Xin Liu, Zaiwen Wen, and Ya xiang Yuan. A brief introduction to manifold optimization. *Journal of the Operations Research Society of China*, 8:199–248, 2020. doi: 10.1007/s40305-020-00295-9.

- Noémie Jaquier, Leonel Rozo, Sylvain Calinon, and Mathias Bürger. Bayesian optimization meets Riemannian manifolds in robot learning. In *Conference on Robot Learning*, pages 233–246. PMLR, 2020.
- I.T. Jolliffe. *Principal Component Analysis*. Springer series in statistics. Springer-Verlag, 1986. ISBN 9780387962696.
- Alex Krizhevsky. Learning multiple layers of features from tiny images. Technical report, University of Toronto, 2009.
- Harold W. Kuhn. A note on Fermat’s problem. *Mathematical Programming*, 4(1):98–107, 1973.
- Christian Kümmerle, Claudio Mayrink Verdun, and Dominik Stöger. Iteratively reweighted least squares for basis pursuit with global linear convergence rate. In *Neural Information Processing Systems*, 2020.
- Gilad Lerman and Tyler Maunu. Fast, robust and non-convex subspace recovery. *Information and Inference: A Journal of the IMA*, 7(2):277–336, 2018a.
- Gilad Lerman and Tyler Maunu. An overview of robust subspace recovery. *Proceedings of the IEEE*, 106(8):1380–1410, 2018b.
- Gilad Lerman and Teng Zhang.  $l_p$ -recovery of the most significant subspace among multiple subspaces with outliers. *Constructive Approximation*, 40(3):329–385, 2014.
- Gilad Lerman, Michael B McCoy, Joel A Tropp, and Teng Zhang. Robust computation of linear models by convex relaxation. *Foundations of Computational Mathematics*, 15(2):363–410, 2015.
- Gilad Lerman, Feng Yu, and Teng Zhang. Theoretical guarantees for the subspace-constrained Tyler’s estimator, 2024. URL <https://arxiv.org/abs/2403.18658>.
- Jiaxiang Li, Shiqian Ma, and Tejes Srivastava. A riemannian alternating direction method of multipliers. *Mathematics of Operations Research*, 2024.
- Tao Li, Lei Tan, Zhehao Huang, Qinghua Tao, Yipeng Liu, and Xiaolin Huang. Low dimensional trajectory hypothesis is true: DNNs can be trained in tiny subspaces. *IEEE Transactions on Pattern Analysis and Machine Intelligence*, 45(3):3411–3420, 2022.
- Xingguo Li, Junwei Lu, Raman Arora, Jarvis Haupt, Han Liu, Zhaoran Wang, and Tuo Zhao. Symmetry, saddle points, and global optimization landscape of nonconvex matrix factorization. *IEEE Transactions on Information Theory*, 65(6):3489–3514, 2019.

- N. Locantore, J. S. Marron, D. G. Simpson, N. Tripoli, J. T. Zhang, K. L. Cohen, Graciela Boente, Ricardo Fraiman, Babette Brumback, Christophe Croux, Jianqing Fan, Alois Kneip, John I. Marden, Daniel Peña, Javier Prieto, Jim O. Ramsay, Mariano J. Valderrama, Ana M. Aguilera, N. Locantore, J. S. Marron, D. G. Simpson, N. Tripoli, J. T. Zhang, and K. L. Cohen. Robust principal component analysis for functional data. *Test*, 8(1):1–73, 1999.
- R.A. Maronna, D.R. Martin, and V.J. Yohai. *Robust Statistics: Theory and Methods*. Wiley Series in Probability and Statistics. Wiley, 2006. ISBN 9780470010921.
- Tyler Maunu and Gilad Lerman. Robust subspace recovery with adversarial outliers, 2019. URL <https://arxiv.org/abs/1904.03275>.
- Tyler Maunu, Teng Zhang, and Gilad Lerman. A well-tempered landscape for non-convex robust subspace recovery. *Journal of Machine Learning Research*, 20(37), 2019.
- Karl Pearson. LIII. on lines and planes of closest fit to systems of points in space. *The London, Edinburgh, and Dublin Philosophical Magazine and Journal of Science*, 2(11):559–572, 1901.
- Liangzu Peng, Christian Kümmeler, and René Vidal. Global linear and local superlinear convergence of irls for non-smooth robust regression. In *Proceedings of the 36th International Conference on Neural Information Processing Systems*. Curran Associates Inc., 2024. ISBN 9781713871088.
- Mostafa Rahmani and George K Atia. Coherence pursuit: Fast, simple, and robust principal component analysis. *IEEE Transactions on Signal Processing*, 65(23):6260–6275, 2017.
- Umut Simsekli, Levent Sagun, and Mert Gurbuzbalaban. A tail-index analysis of stochastic gradient noise in deep neural networks. In *International Conference on Machine Learning*, pages 5827–5837. PMLR, 2019.
- Ying Sun, Prabhu Babu, and Daniel P Palomar. Majorization-minimization algorithms in signal processing, communications, and machine learning. *IEEE Transactions on Signal Processing*, 65(3):794–816, 2016.
- David E Tyler. A distribution-free M-estimator of multivariate scatter. *The Annals of Statistics*, pages 234–251, 1987.
- Bart Vandereycken. Low-rank matrix completion by Riemannian optimization. *SIAM Journal on Optimization*, 23(2):1214–1236, 2013.
- Roman Vershynin. Introduction to the non-asymptotic analysis of random matrices. *arXiv preprint arXiv:1011.3027*, 2010.

- Roman Vershynin. *High-Dimensional Probability: An Introduction with Applications in Data Science*. Cambridge Series in Statistical and Probabilistic Mathematics. Cambridge University Press, 2018. ISBN 9781108415194.
- Peng Wang, Huijie Zhang, Zekai Zhang, Siyi Chen, Yi Ma, and Qing Qu. Diffusion model learns low-dimensional distributions via subspace clustering. In *NeurIPS 2024 Workshop on Mathematics of Modern Machine Learning*, 2024.
- Endre Weiszfeld. Sur le point pour lequel la somme des distances de  $n$  points donnés est minimum. *Tohoku Mathematical Journal, First Series*, 43:355–386, 1937.
- Ami Wiesel and Teng Zhang. Structured robust covariance estimation. *Foundations and Trends® in Signal Processing*, 8(3):127–216, 2015. ISSN 1932-8346. doi: 10.1561/20000000053.
- Huan Xu, Constantine Caramanis, and Sujay Sanghavi. Robust pca via outlier pursuit. *IEEE Transactions on Information Theory*, 58(5):3047–3064, 2012.
- Yongyi Yang, David P Wipf, et al. Transformers from an optimization perspective. *Advances in Neural Information Processing Systems*, 35:36958–36971, 2022.
- Feng Yu, Teng Zhang, and Gilad Lerman. A subspace-constrained Tyler’s estimator and its applications to structure from motion. In *Proceedings of the IEEE/CVF Conference on Computer Vision and Pattern Recognition*, pages 14575–14584, 2024.
- Teng Zhang. Robust subspace recovery by Tyler’s M-estimator. *Information and Inference: A Journal of the IMA*, 5(1):1–21, 2016.
- Teng Zhang and Gilad Lerman. A novel M-estimator for robust PCA. *Journal of Machine Learning Research*, 15(23):749–808, 2014.
- Teng Zhang, Arthur Szlam, and Gilad Lerman. Median k-flats for hybrid linear modeling with many outliers. In *2009 IEEE 12th International Conference on Computer Vision Workshops, ICCV Workshops*, pages 234–241, 2009. doi: 10.1109/ICCVW.2009.5457695.
- Pan Zhou, Jiashi Feng, Chao Ma, Caiming Xiong, Steven Chu Hong Hoi, et al. Towards theoretically understanding why SGD generalizes better than Adam in deep learning. *Advances in Neural Information Processing Systems*, 33:21285–21296, 2020.
- Zhihui Zhu, Yifan Wang, Daniel Robinson, Daniel Naiman, René Vidal, and Manolis Tsakiris. Dual principal component pursuit: Improved analysis and efficient algorithms. In S. Bengio,

H. Wallach, H. Larochelle, K. Grauman, N. Cesa-Bianchi, and R. Garnett, editors, *Advances in Neural Information Processing Systems*, volume 31. Curran Associates, Inc., 2018.